

A LOCKING-FREE MIXED VIRTUAL ELEMENT DISCRETIZATION FOR THE ELASTICITY EIGENVALUE PROBLEM*

FELIPE LEPE[†] AND GONZALO RIVERA[‡]

Abstract. In this paper, we introduce a mixed virtual element method to approximate the eigenvalues and eigenfunctions of the two-dimensional elasticity eigenvalue problem. Under standard assumptions on the meshes, we prove the convergence of the discrete solution operator to the continuous one as the mesh size tends to zero. Using the theory of compact operators, we analyze the convergence of the method and derive error estimates for both the eigenvalues and eigenfunctions. We validate our theoretical results with a series of numerical tests, in which we compute convergence orders and show that the method is locking-free and capable of accurately approximating the spectrum independently of the shape of the polygons on the meshes.

Key words. eigenvalue problems, virtual elements, mixed formulations, elasticity equations, convergence, a priori error estimates

AMS subject classifications. 35M30, 65N12, 65N15, 65N25, 65N30, 74B05, 74S99

1. Introduction. The development of numerical methods to approximate the elasticity equations, and particularly the elasticity eigenvalue problem, has been widely studied in recent years. Different primal and mixed formulations, together with their corresponding discretizations, have emerged to address this problem. A non-exhaustive list of contributions and the references therein is available in [10, 14, 15, 16, 24, 25, 35]. Here, the load and eigenvalue problems have been analyzed using different techniques with the aim of approximating the solutions while taking into account the inherent difficulties of the linear elasticity equations, particularly those related to the locking phenomenon that the Poisson ratio may produce when it is close to 1/2. This issue is important to consider, since if the formulations and numerical methods are not properly designed, instabilities may arise in the approximation of the solutions and, in particular, in the spectrum of the eigenvalue problem. The bibliographical discussion reveals that a suitable alternative to handle the linear elasticity eigenvalue problem is provided by mixed formulations, since these methods are precisely capable of avoiding locking. The aim of this paper is to present a mixed virtual element method (VEM) to approximate the spectrum of the elasticity operator. The application of VEM to eigenvalue problems is in constant development, as observed in the following non-exhaustive list [1, 2, 26, 27, 29, 30, 34], where the VEM has been used to approximate eigenvalues and eigenfunctions of partial differential equations in different contexts. In particular, for the elasticity eigenvalue problem, we highlight [3, 32] as contributions employing the VEM. Despite the fact that there is an important amount of contributions where the VEM is analyzed for eigenvalue problems, the literature regarding mixed formulations and their VEM approximations remains scarce where [22, 23, 26, 28, 30, 31] are our main references on this topic where the research is in constant development. Particularly, mixed formulations based on ten-

*Submitted to the editors DATE.

Funding: The first author was partially supported by DIUBB through project 2120173 GI/C Universidad del Bío-Bío (Chile). The second author was supported by ANID-Chile through FONDECYT project 1231619 (Chile).

[†]GIMNAP-Departamento de Matemática, Universidad del Bío - Bío, Casilla 5-C, Concepción, Chile. flepe@ubiobio.cl.

[‡]Departamento de Ciencias Exactas, Universidad de Los Lagos, Casilla 933, Osorno, Chile. gonzalo.rivera@ulagos.cl.

serial fields and their respective tensorial version of VEM has only an application for the Stokes eigenvalue problem [23]. This paper reveals that a pseudostress tensor is a suitable alternative to approximate the spectrum of the eigenvalue problem since with only this unknown, it is possible to recover other quantities as the velocity and pressure via a simple post-process. The task now is to analyze a similar approach for the elasticity eigenvalue problem.

In this paper we study a mixed VEM for the elasticity eigenproblem considering the formulation provided in [15]. This mixed formulation, originally proposed for the load problem, was analyzed for the eigenvalue problem in [19] under a finite element scheme, where a priori error estimates were obtained. This formulation shows that it is possible to compute the spectrum of the elasticity eigenproblem while avoiding the locking that arises in the primal formulation. Hence, we expect that for the VEM the results can be as accurate as those obtained with the finite element scheme, while allowing the use of general polygonal meshes to discretize different domains. Here the main difference with the FEM setting is that under the VEM approach, some terms are computable via the degrees of freedom whereas other terms are not and hence, polynomial projections are needed. For the mixed load problem, [13] describes rigorously this analysis and some of these results are necessary for the spectral problem. On one hand, the regularity of the load problems implies the compactness of the solution operator, which in our case, will be compact and as a consequence, the well known theory for compact operators of [4] is applied in order to conclude convergence of the method. However, for the error estimates of eigenvalues and eigenfunctions, the regularity of the load problem is not enough, because the eigenfunctions are of different nature and hence, these error estimates must be concluded with the corresponding regularity. Other important (and not minor) issue to address is the influence of the Lamé constants on the spectrum. As is stated in [21], the Lamé constant λ makes the spectrum of the elasticity problem change, implying to consider families of spectrums depending on λ . In fact, when this Lamé constant when blows up (namely, the Poisson ratio tends to $1/2$), forces to analyze the limit problem which coincides with the Stokes eigenvalue problem. This means that the spectrum of elasticity converges the spectrum of Stokes when $\lambda \rightarrow \infty$. It is for this reason that a mixed formulation is a suitable way to analyze the nearly incompressible and perfectly incompressible regimes for elasticity. This was also studied in [19] in two and three dimensions with a finite element method. Now we are interested in investigating if the VEM is capable to capture the spectrum of elasticity with polygonal meshes and what effects cause the stabilization of the VEM with respect to the spurious eigenmodes and the convergence orders.

1.1. Notations and preliminaries. Given any Hilbert space X , let X^2 and \mathbb{X} denote, respectively, the space of vectors and tensors with entries in X . In particular, \mathbb{I} is the identity matrix of $\mathbb{R}^{2 \times 2}$, and $\mathbf{0}$ denotes a generic null vector or tensor. Given $\boldsymbol{\tau} := (\tau_{ij})$ and $\boldsymbol{\sigma} := (\sigma_{ij}) \in \mathbb{R}^{2 \times 2}$, we define, as usual, the transpose tensor $\boldsymbol{\tau}^\mathbf{t} := (\tau_{ji})$, the trace $\text{tr } \boldsymbol{\tau} := \sum_{i=1}^2 \tau_{ii}$ and the tensor inner product $\boldsymbol{\tau} : \boldsymbol{\sigma} := \sum_{i,j=1}^2 \tau_{ij} \sigma_{ij}$.

Let Ω be a polygonal Lipschitz bounded domain of \mathbb{R}^2 with boundary $\partial\Omega$. For $s \geq 0$, $\|\cdot\|_{s,\Omega}$ stands indistinctly for the norm of the Hilbertian Sobolev spaces $H^s(\Omega)$, $H^s(\Omega)^2$ or $\mathbb{H}^s(\Omega)$ for scalar, vectorial and tensorial fields, respectively, with the convention $H^0(\Omega) := L^2(\Omega)$, $H^0(\Omega)^2 = L^2(\Omega)^2$ and $\mathbb{H}^0(\Omega) := \mathbb{L}^2(\Omega)$. We also define the Hilbert space $\mathbb{H}(\mathbf{div}; \Omega) := \{\boldsymbol{\tau} \in \mathbb{L}^2(\Omega) : \mathbf{div } \boldsymbol{\tau} \in L^2(\Omega)^2\}$, whose norm is given by $\|\boldsymbol{\tau}\|_{\mathbf{div},\Omega}^2 := \|\boldsymbol{\tau}\|_{0,\Omega}^2 + \|\mathbf{div } \boldsymbol{\tau}\|_{0,\Omega}^2$.

2. The model problem. Let us consider an open and bounded domain $\Omega \subset \mathbb{R}^2$, with Lipschitz boundary $\partial\Omega$. We are interested in the elasticity eigenvalue problem: Find $\kappa \in \mathbb{R}^+$ and the pair $(\boldsymbol{\sigma}, \mathbf{u})$ such that

$$(2.1) \quad \begin{cases} \boldsymbol{\sigma} = 2\mu\boldsymbol{\varepsilon}(\mathbf{u}) + \lambda \operatorname{tr}(\boldsymbol{\varepsilon}(\mathbf{u}))\mathbb{I} & \text{in } \Omega, \\ \operatorname{div} \boldsymbol{\sigma} = -\kappa\mathbf{u} & \text{in } \Omega, \\ \mathbf{u} = \mathbf{0} & \text{on } \partial\Omega, \end{cases}$$

where \mathbf{u} represents the displacement of the elastic structure, $\boldsymbol{\sigma}$ is the Cauchy tensor, λ and μ are the positive Lamé constants defined by

$$\lambda := \frac{E\nu}{(1+\nu)(1-2\nu)} \quad \text{and} \quad \mu := \frac{E}{2(1+\nu)},$$

where E is the Young's modulus and ν is the Poisson ratio. Let us remark that on our paper, we are considering ordinary materials, implying that $\nu \in [0, 1/2]$. Additionally, $\mathbb{I} \in \mathbb{R}^{2 \times 2}$ is the identity matrix, and $\boldsymbol{\varepsilon}(\mathbf{u})$ represents the tensor of small deformations, given by $\boldsymbol{\varepsilon}(\mathbf{u}) := \frac{1}{2}(\nabla\mathbf{u} + (\nabla\mathbf{u})^\dagger)$, where \dagger is the transpose operator.

We describe the model problem of interest. From the first equation of (2.1) we have the following identity

$$\operatorname{div} \boldsymbol{\sigma} = 2\mu \operatorname{div} \boldsymbol{\varepsilon}(\mathbf{u}) + \lambda \nabla \operatorname{div} \mathbf{u} = \mu \Delta \mathbf{u} + (\lambda + \mu) \nabla \operatorname{div} \mathbf{u}.$$

Now we introduce the so called pseudostress tensor (see [15] for instance), defined by

$$\boldsymbol{\rho} := \mu \nabla \mathbf{u} + (\lambda + \mu) \operatorname{div} \mathbf{u} \mathbb{I} = \mu \nabla \mathbf{u} + (\lambda + \mu) \operatorname{tr}(\nabla \mathbf{u}) \mathbb{I}.$$

Hence, following the same steps described in [19], we obtain the following system

$$\begin{cases} \frac{1}{\mu} \left\{ \boldsymbol{\rho} - \frac{\lambda + \mu}{2\lambda + 3\mu} \operatorname{tr}(\boldsymbol{\rho}) \mathbb{I} \right\} = \nabla \mathbf{u} & \text{in } \Omega, \\ \operatorname{div} \boldsymbol{\rho} = -\kappa \mathbf{u} & \text{in } \Omega, \\ \mathbf{u} = \mathbf{0} & \text{on } \partial\Omega. \end{cases}$$

whose variational formulation is: Find $\kappa \in \mathbb{R}$ and $\mathbf{0} \neq (\boldsymbol{\rho}, \mathbf{u}) \in \mathbb{H} \times \mathbf{Q}$, such that

$$(2.2) \quad \begin{cases} a(\boldsymbol{\rho}, \boldsymbol{\tau}) + b(\boldsymbol{\tau}, \mathbf{u}) = 0 & \forall \boldsymbol{\tau} \in \mathbb{H}, \\ b(\boldsymbol{\rho}, \mathbf{v}) = -\kappa c(\mathbf{u}, \mathbf{v}) & \forall \mathbf{v} \in \mathbf{Q}, \end{cases}$$

where $\mathbb{H} := \mathbb{H}(\operatorname{div}; \Omega)$, $\mathbf{Q} := L^2(\Omega)^2$, is defined by

$$a(\boldsymbol{\xi}, \boldsymbol{\tau}) := \frac{1}{\mu} \int_{\Omega} \boldsymbol{\xi} : \boldsymbol{\tau} - \frac{\lambda + \mu}{\mu(2\lambda + 3\mu)} \int_{\Omega} \operatorname{tr}(\boldsymbol{\xi}) \operatorname{tr}(\boldsymbol{\tau}) \quad \forall \boldsymbol{\xi}, \boldsymbol{\tau} \in \mathbb{H},$$

the forms $b : \mathbb{H} \times \mathbf{Q} \rightarrow \mathbb{R}$ and $c : \mathbf{Q} \times \mathbf{Q} \rightarrow \mathbb{R}$ are defined, respectively, by

$$b(\boldsymbol{\tau}, \mathbf{v}) := \int_{\Omega} \mathbf{v} \cdot \operatorname{div} \boldsymbol{\tau} \quad \forall \boldsymbol{\tau} \in \mathbb{H}, \forall \mathbf{v} \in \mathbf{Q}, \quad \text{and} \quad c(\mathbf{w}, \mathbf{v}) := \int_{\Omega} \mathbf{u} \cdot \mathbf{w} \quad \forall \mathbf{w}, \mathbf{v} \in \mathbf{Q}.$$

Let $\boldsymbol{\tau} \in \mathbb{H}$. The deviator of $\boldsymbol{\tau}$, defined by $\boldsymbol{\tau}^d := \boldsymbol{\tau} - \frac{1}{2} \operatorname{tr}(\boldsymbol{\tau}) \mathbb{I}$, allows us to rewrite $a(\cdot, \cdot)$ as follows

$$a(\boldsymbol{\xi}, \boldsymbol{\tau}) := \frac{1}{\mu} \int_{\Omega} \boldsymbol{\xi}^d : \boldsymbol{\tau}^d + \frac{1}{4\lambda + 6\mu} \int_{\Omega} \operatorname{tr}(\boldsymbol{\xi}) \operatorname{tr}(\boldsymbol{\tau}) \quad \forall \boldsymbol{\xi}, \boldsymbol{\tau} \in \mathbb{H},$$

where the presence of the coefficient λ is now on the denominator, leading to estimates that will be independent of this parameter.

For the analysis of the mixed formulation it is convenient to decompose the space \mathbb{H} as follows $\mathbb{H} := \mathbb{H}_0 \oplus \mathbb{R}\mathbb{I}$, where

$$\mathbb{H}_0 := \left\{ \boldsymbol{\tau} \in \mathbb{H} : \int_{\Omega} \operatorname{tr}(\boldsymbol{\tau}) = 0 \right\}.$$

Note that for any $\boldsymbol{\xi} \in \mathbb{H}$ there exists a unique $\boldsymbol{\xi}_0 \in \mathbb{H}_0$ and $d := \frac{1}{2|\Omega|} \int_{\Omega} \operatorname{tr}(\boldsymbol{\xi}) \in \mathbb{R}$ such that $\boldsymbol{\xi} = \boldsymbol{\xi}_0 + d\mathbb{I}$. Hence, problem (2.2) is now stated as follows: Find $\kappa \in \mathbb{R}^+$ and $(\mathbf{0}, \mathbf{0}) \neq (\boldsymbol{\rho}, \mathbf{u}) \in \mathbb{H}_0 \times \mathbf{Q}$, such that

$$(2.3) \quad \begin{cases} a(\boldsymbol{\rho}, \boldsymbol{\tau}) + b(\boldsymbol{\tau}, \mathbf{u}) &= 0 & \forall \boldsymbol{\tau} \in \mathbb{H}_0, \\ b(\boldsymbol{\rho}, \mathbf{v}) &= -\kappa c(\mathbf{u}, \mathbf{v}) & \forall \mathbf{v} \in \mathbf{Q}, \end{cases}$$

We note that, instead of seeking the eigenfunction in the space \mathbb{H} , we may equivalently consider it in the space \mathbb{H}_0 . This follows from [15, Lemma 2.1] and, in particular, from the fact that we are working with a vanishing Dirichlet boundary condition. For this reason, we define the following solution operator:

$$\boldsymbol{T} : \mathbf{Q} \rightarrow \mathbf{Q}, \quad \mathbf{f} \mapsto \boldsymbol{T}\mathbf{f} := \widehat{\mathbf{u}}, \quad \boldsymbol{S} : \mathbf{Q} \rightarrow \mathbb{H}_0, \quad \mathbf{f} \mapsto \boldsymbol{S}\mathbf{f} := \widehat{\boldsymbol{\rho}},$$

where the pair $(\widehat{\boldsymbol{\rho}}, \widehat{\mathbf{u}})$ is the solution of the following source problem

$$(2.4) \quad \begin{cases} a(\widehat{\boldsymbol{\rho}}, \boldsymbol{\tau}) + b(\boldsymbol{\tau}, \widehat{\mathbf{u}}) &= 0 & \forall \boldsymbol{\tau} \in \mathbb{H}_0, \\ b(\widehat{\boldsymbol{\rho}}, \mathbf{v}) &= -c(\mathbf{f}, \mathbf{v}) & \forall \mathbf{v} \in \mathbf{Q}. \end{cases}$$

The following technical result is needed for the control of the L^2 -norm of the deviator (see [8, Proposition 9.1.1])

$$\|\boldsymbol{\tau}\|_{0,\Omega}^2 \leq C \|\boldsymbol{\tau}^d\|_{0,\Omega}^2 + \|\operatorname{div} \boldsymbol{\tau}\|_{0,\Omega}^2 \quad \forall \boldsymbol{\tau} \in \mathbb{H}_0.$$

It is straightforward to verify that $a(\cdot, \cdot)$ and $b(\cdot, \cdot)$ are bounded bilinear forms. Furthermore, if $\mathbb{V} := \{\boldsymbol{\tau} \in \mathbb{H}_0 : \operatorname{div} \boldsymbol{\tau} = \mathbf{0}\}$ is the kernel of $b(\cdot, \cdot)$, it is easy to check the existence of a constant $\alpha > 0$ independent of λ but depending on μ , such that

$$a(\boldsymbol{\tau}, \boldsymbol{\tau}) \geq \alpha \|\boldsymbol{\tau}\|_{\operatorname{div},\Omega}^2 \quad \forall \boldsymbol{\tau} \in \mathbb{V}.$$

Moreover, the following inf-sup condition for $b(\cdot, \cdot)$ holds (see [15, Theorem 2.1]),

$$\sup_{\mathbf{0} \neq \boldsymbol{\tau} \in \mathbb{H}_0} \frac{b(\boldsymbol{\tau}, \mathbf{v})}{\|\boldsymbol{\tau}\|_{\operatorname{div},\Omega}} \geq \beta \|\mathbf{v}\|_{0,\Omega} \quad \forall \mathbf{v} \in \mathbf{Q}.$$

Hence, according to the Babuška–Brezzi theory (see [8] for a comprehensive review), problem (2.4) is well posed and there exists a constant $C > 0$, independent of λ , such that

$$\|\widehat{\boldsymbol{\rho}}\|_{\operatorname{div},\Omega} + \|\widehat{\mathbf{u}}\|_{0,\Omega} \leq C \|\mathbf{f}\|_{0,\Omega}.$$

This implies that \boldsymbol{T} and \boldsymbol{S} are well defined. Furthermore, it is straightforward to verify that \boldsymbol{T} is self-adjoint with respect to the $L^2(\Omega)$ inner product and that

$(\kappa, (\boldsymbol{\rho}, \mathbf{u})) \in \mathbb{R}^+ \times \mathbb{H}_0 \times \mathbf{Q}$ solves (2.2) if and only if (ζ, \mathbf{u}) is an eigenpair of \mathbf{T} with $\zeta \neq 0$ and $\mathbf{u} \neq \mathbf{0}$.

Now we present an additional regularity for the eigenfunctions of \mathbf{T} which is derived from the classic regularity results for linear elasticity (see [17]), together with a standard bootstrap argument.

LEMMA 2.1. *The following statements hold:*

- For all $\mathbf{f} \in \mathbf{Q}$, if $(\widehat{\boldsymbol{\rho}}, \widehat{\mathbf{u}}) \in \mathbb{H}_0 \times \mathbf{Q}$ solves problem (2.4), there exists $\widehat{s} \in (0, 1]$ and $\widehat{C} > 0$ that depend on Ω and λ such that $\mathbf{u} \in \mathbf{H}^{1+\widehat{s}}(\Omega)^2$, $\boldsymbol{\rho} \in \mathbb{H}^{\widehat{s}}(\Omega)$ and $\mathbf{div} \widehat{\boldsymbol{\rho}} \in \mathbf{H}^{1+\widehat{s}}(\Omega)^2$ and satisfies the following estimate

$$\|\widehat{\boldsymbol{\rho}}\|_{s,\Omega} + \|\mathbf{div} \widehat{\boldsymbol{\rho}}\|_{1+s,\Omega} + \|\widehat{\mathbf{u}}\|_{1+s,\Omega} \leq \widehat{C} \|\mathbf{f}\|_{0,\Omega} \quad \forall s \in (0, \widehat{s}).$$

- Let \mathbf{u} be an eigenfunction of \mathbf{T} associated to an eigenvalue κ . Then, for all $r > 0$, we have that $\mathbf{u} \in \mathbf{H}^{1+r}(\Omega)^2$. Also, there exists a constant $\widehat{C} > 0$ which in principle depends on λ and on the eigenvalue κ such that

$$\|\boldsymbol{\rho}\|_{r,\Omega} + \|\mathbf{div} \boldsymbol{\rho}\|_{1+r,\Omega} + \|\mathbf{u}\|_{1+r,\Omega} \leq \widehat{C} \|\mathbf{u}\|_{0,\Omega}.$$

Remark 2.2. As is discussed in [21, Section 2], the dependency λ on the regularity exponents s and r of the previous lemma is not completely evident since in our numerical experiments (cf. Section 5), even for the perfectly incompressible elasticity eigenvalue problem ($\lambda = \infty$), our method is capable to attain the expected convergence orders. This leads us to consider the following assumption along our paper:

Assumption 2.3. Constants \widehat{s} , \widehat{r} , and \widehat{C} in Lemma 2.1 are independent of λ .

Remark 2.4. The perfectly incompressible has been also studied in [19, subsection 2.1] where has been proved that for formulation (2.3) its limits corresponds to the Stokes eigenvalue problem. Hence, the spectrum of (2.3) converges to the spectrum of Stokes as $\lambda \rightarrow +\infty$. See [19, Lemma 2.2] and [19, Theorem 2.2] for further details.

The regularity of Lemma 2.1 allows us to conclude that \mathbf{T} is a compact operator, thanks to the compact inclusion $\mathbf{H}^{1+s}(\Omega)^2 \hookrightarrow \mathbf{Q}$ and hence, the following spectral characterization of \mathbf{T} holds.

THEOREM 2.5 (Spectral characterization of \mathbf{T}). *The spectrum of \mathbf{T} satisfies $\text{sp}(\mathbf{T}) = \{0\} \cup \{\zeta_k\}_{k \in \mathbb{N}}$, where $\{\zeta_k\}_{k \in \mathbb{N}}$ is a sequence of real positive eigenvalues which converges to zero, repeated according their respective multiplicities.*

To end this section, we define the following continuous bilinear form

$$A((\boldsymbol{\rho}, \mathbf{u}), (\boldsymbol{\tau}, \mathbf{v})) := a(\boldsymbol{\rho}, \boldsymbol{\tau}) + b(\boldsymbol{\tau}, \mathbf{u}) + b(\boldsymbol{\rho}, \mathbf{v}) \quad \forall \boldsymbol{\rho}, \boldsymbol{\tau} \in \mathbb{H}, \forall \mathbf{v}, \mathbf{u} \in \mathbf{Q},$$

With this form $A(\cdot, \cdot)$ at hand, problems (2.2) and (2.4) can be rewritten in a more simple way in order to prove some results.

3. The virtual element approximation. In this section, we present the formulation and the theoretical analysis of a virtual element method for approximating the solutions of problem (2.2). To this end, we introduce a set of assumptions and definitions that are required to conduct the analysis within the virtual element framework

3.1. Assumptions on the mesh and virtual spaces. Let $\{\mathcal{T}_h(\Omega)\}_{h>0}$ be a sequence of decompositions of Ω into elements E , We suppose that each $\{\mathcal{T}_h(\Omega)\}_{h>0}$ is built according with the procedure described below.

The polygonal domain Ω is partitioned into a polygonal mesh \mathcal{T}_h that is *regular*, in the sense that there exist positive constants c, η such that

1. each edge $e \in \partial E$ has a length $h_e \geq c h_E$, where h_E denotes the diameter of E ;
2. each polygon E in the mesh is star-shaped with respect to a ball of radius ηh_E .

3.1.1. Virtual space to approximate the pseudostress. We summarize the construction of the VEM spaces that we require. For further details we refer to [12, Subsection 3.2]. Given a geometric object \mathcal{O} of dimension $d \in \{1, 2\}$, as an edge or an element, with barycenter $x_{\mathcal{O}}$ and diameter $h_{\mathcal{O}}$, we consider the following set of normalized monomials on \mathcal{O} (of dimension $k+1$ for $d=1$ and $(k+1)(k+2)/2$ for $d=2$)

$$\mathcal{M}_k(\mathcal{O}) := \left\{ q \mid q := \left(\frac{\mathbf{x} - \mathbf{x}_{\mathcal{O}}}{h_{\mathcal{O}}} \right)^{\boldsymbol{\alpha}} \text{ for } \boldsymbol{\alpha} \in \mathbb{N}^d \text{ with } |\boldsymbol{\alpha}| \leq k \right\},$$

where for a multi-index $\boldsymbol{\alpha} := (\alpha_1, \dots, \alpha_d)$, we denote, as usual, $|\boldsymbol{\alpha}| := \alpha_1 + \dots + \alpha_d$ and $\mathbf{x}^{\boldsymbol{\alpha}} := x_1^{\alpha_1} \dots x_d^{\alpha_d}$. It is easy to check that $\mathcal{M}_k(\mathcal{O})$ is a basis of $\mathbf{P}_k(\mathcal{O})$ (see [5] for more details).

For each integer $k \geq 0$ and for each $E \in \mathcal{T}_h$, we introduce the following local virtual element space of order k :

$$\mathbb{H}_h^E := \left\{ \boldsymbol{\tau} \in \mathbb{H}(\mathbf{div}; E) \cap \mathbb{H}(\mathbf{rot}; E) : \boldsymbol{\tau} \mathbf{n} \in \mathbf{P}_k(e) \quad \forall e \subset \partial E, \right. \\ \left. \mathbf{div} \boldsymbol{\tau} \in \mathbf{P}_k(E), \quad \mathbf{rot} \boldsymbol{\tau} \in \mathbf{P}_{k-1}(E) \right\},$$

and let us define the

$$\mathcal{M}_k(\mathcal{O}) := \left\{ (q, 0)^t : q \in \mathcal{M}_k(\mathcal{O}) \right\} \cup \left\{ (0, q)^t : q \in \mathcal{M}_k(\mathcal{O}) \right\},$$

and

$$\mathcal{H}_k^{\perp} := \left\{ \begin{pmatrix} \mathbf{q} \\ 0 \end{pmatrix} : \mathbf{q} \in \mathcal{H}_k^{\perp}(E) \right\} \cup \left\{ \begin{pmatrix} 0 \\ \mathbf{q} \end{pmatrix} : \mathbf{q} \in \mathcal{H}_k^{\perp}(E) \right\}.$$

It is easy to check that the space (3.1.1) is unisolvent respect to the following degrees of freedom

$$(3.1) \quad \int_e \boldsymbol{\tau} \mathbf{n} \cdot \mathbf{q} \quad \forall \mathbf{q} \in \mathcal{M}_k(e) \quad \forall \text{edge } e \in \mathcal{T}_h,$$

$$(3.2) \quad \int_E \boldsymbol{\tau} : \nabla \mathbf{q} \quad \forall \mathbf{q} \in \mathcal{M}_k(E) \setminus \{(1, 0)^t, (0, 1)^t\} \quad \forall E \in \mathcal{T}_h,$$

$$(3.3) \quad \int_E \boldsymbol{\tau} : \boldsymbol{\rho} \quad \forall \boldsymbol{\rho} \in \mathcal{H}_k^{\perp}(E) \quad \forall E \in \mathcal{T}_h.$$

Now, for every decomposition \mathcal{T}_h of Ω into simple polygons E , we define the global virtual element space

$$\mathbb{H}_h := \left\{ \boldsymbol{\tau}_h \in \mathbb{H} : \boldsymbol{\tau}_h|_E \in \mathbb{H}_h^E \text{ for all } E \in \mathcal{T}_h \right\},$$

and the discrete counterpart of \mathbb{H}_0 is defined by

$$\mathbb{H}_{0,h} := \left\{ \boldsymbol{\tau}_h \in \mathbb{H}_h : \int_{\Omega} \text{tr}(\boldsymbol{\tau}_h) = 0 \right\}.$$

Observe that $\int_{\Omega} \text{tr}(\boldsymbol{\tau})$ is computable from the degrees of freedom. Indeed, if $\mathbf{x} \in \mathbf{P}_k(E)$ we have

$$\begin{aligned} \int_{\Omega} \text{tr}(\boldsymbol{\tau}) &= \sum_{E \in \mathcal{T}_h} \int_K \text{tr}(\boldsymbol{\tau}) = \sum_{E \in \mathcal{T}_h} \int_K \boldsymbol{\tau} : \mathbb{I} = \sum_{E \in \mathcal{T}_h} \int_K \boldsymbol{\tau} : \nabla \mathbf{x} \\ &= \sum_{E \in \mathcal{T}_h} \left(- \int_K \mathbf{div} \boldsymbol{\tau} \cdot \mathbf{x} + \int_{\partial E} \boldsymbol{\tau} \mathbf{n} \cdot \mathbf{x} \right), \end{aligned}$$

3.2. Discrete bilinear forms. Let us begin by writing the bilinear forms elementwise as follows

$$a(\boldsymbol{\rho}, \boldsymbol{\tau}) = \sum_{E \in \mathcal{T}_h} a^E(\boldsymbol{\rho}, \boldsymbol{\tau}) = \sum_{E \in \mathcal{T}_h} \frac{1}{\mu} \int_E \boldsymbol{\rho}^d : \boldsymbol{\tau}^d + \frac{1}{4\lambda + 6\mu} \int_E \text{tr}(\boldsymbol{\rho}) \text{tr}(\boldsymbol{\tau}),$$

and

$$b(\boldsymbol{\tau}, \mathbf{v}) = \sum_{E \in \mathcal{T}_h} b^E(\boldsymbol{\tau}, \mathbf{v}) = \sum_{E \in \mathcal{T}_h} \int_E \mathbf{v} \cdot \mathbf{div} \boldsymbol{\tau}.$$

We denote by \mathcal{P}_k^h the L^2 -orthogonal projection onto \mathcal{Q}_h as follows

$$\mathcal{P}_k^h : L^2(\Omega)^2 \rightarrow \mathcal{Q}_h := \{\mathbf{q} \in L^2(\Omega)^2 \mid \mathbf{q}|_E \in \mathbf{P}_k(E) \quad \forall E \in \mathcal{T}_h\},$$

which for $\mathbf{v} \in L^2(\Omega)^2$ satisfies

$$\int_E \mathcal{P}_k^h(\mathbf{v}) \cdot \mathbf{q} = \int_E \mathbf{v} \cdot \mathbf{q} \quad \forall E \in \mathcal{T}_h, \quad \forall \mathbf{q} \in \mathbf{P}_k(E).$$

Observe that $\mathcal{P}_k^h(\mathbf{v})|_E = \mathcal{P}_k^h(\mathbf{v}|_E)$. Also, for $m \in \{0, 1, \dots, k+1\}$, this operator satisfies the following error estimate (see [11] for further details),

$$\|\mathbf{v} - \mathcal{P}_k^h \mathbf{v}\|_{0,E} \leq Ch_E^m |\mathbf{v}|_{m,E}, \quad \forall \mathbf{v} \in \mathbb{H}^m(E)^2, \quad \forall E \in \mathcal{T}_h.$$

Now, inspired by the analysis presented in [12, Subsection 4.1], for each $E \in \mathcal{T}_h$ we define $\Pi_h^E := \mathcal{P}_k^h : L^2(E) \rightarrow \mathbb{P}_k(E)$ be the $L^2(E)$ -orthogonal projector, which satisfies the following properties (see [11, Section 4]):

(A.1) The stability estimate

$$\|\Pi_h^E(\boldsymbol{\tau})\|_{0,E} \leq \|\boldsymbol{\tau}\|_{0,E}, \quad \forall \boldsymbol{\tau} \in \mathbb{H}(\mathbf{div}; E),$$

$$(A.2) \quad \int_E (\Pi_h^E \boldsymbol{\tau})^d : (\Pi_h^E \boldsymbol{\rho})^d = \int_E (\Pi_h^E \boldsymbol{\tau})^d : \boldsymbol{\rho}^d, \quad \text{for all } \boldsymbol{\tau}, \boldsymbol{\rho} \in \mathbb{H}(\mathbf{div}; E), \text{ and}$$

(A.3) given an integer $0 \leq m \leq k+1$, there exists a positive constant C , independent of E , such that

$$\|\boldsymbol{\tau} - \Pi_h^E \boldsymbol{\tau}\|_{0,E} \leq Ch_E^m |\boldsymbol{\tau}|_{m,E}, \quad \forall \boldsymbol{\tau} \in \mathbb{H}^m(E).$$

On the other hand, let $S^E(\cdot, \cdot)$ be any symmetric positive definite bilinear form that satisfies

$$\frac{c_0}{\mu} \int_E \boldsymbol{\tau}_h : \boldsymbol{\tau}_h \leq S^E(\boldsymbol{\tau}_h, \boldsymbol{\tau}_h) \leq \frac{c_1}{\mu} \int_E \boldsymbol{\tau}_h : \boldsymbol{\tau}_h, \quad \forall \boldsymbol{\tau}_h \in \mathbb{H}_h^E,$$

where c_0 and c_1 are positive constants depending on the mesh assumptions. Then, for each element we define the bilinear form

$$a_h^E(\boldsymbol{\sigma}_h, \boldsymbol{\tau}_h) := \frac{1}{\mu} \int_E (\Pi_h^E \boldsymbol{\sigma}_h)^d : (\Pi_h^E \boldsymbol{\tau}_h)^d + \frac{1}{4\lambda + 6\mu} \int_E \operatorname{tr}(\Pi_h^E \boldsymbol{\sigma}_h) \operatorname{tr}(\Pi_h^E \boldsymbol{\tau}_h) + S^E(\boldsymbol{\sigma}_h - \Pi_h^E \boldsymbol{\sigma}_h, \boldsymbol{\tau}_h - \Pi_h^E \boldsymbol{\tau}_h),$$

for $\boldsymbol{\sigma}_h, \boldsymbol{\tau}_h \in \mathbb{H}_h^E$ and, in a natural way,

$$a_h(\boldsymbol{\sigma}_h, \boldsymbol{\tau}_h) := \sum_{E \in \mathcal{T}_h} a_h^E(\boldsymbol{\sigma}_h, \boldsymbol{\tau}_h), \quad \boldsymbol{\sigma}_h, \boldsymbol{\tau}_h \in \mathbb{H}_h^E.$$

The following result states that bilinear form $a_h^E(\cdot, \cdot)$ is consistent and stable.

LEMMA 3.1. *For each $E \in \mathcal{T}_h$ there holds*

$$a_h^E(\boldsymbol{\rho}_h, \boldsymbol{\tau}_h) = a^E(\boldsymbol{\rho}_h, \boldsymbol{\tau}_h) \quad \forall \boldsymbol{\rho}_h \in \mathbb{P}_k(E), \quad \forall \boldsymbol{\tau}_h \in \mathbb{H}_h^E,$$

and there exist constants α_1, α_2 , independent of h and E , such that

$$\alpha_1 a^E(\boldsymbol{\tau}_h, \boldsymbol{\tau}_h) \leq a_h^E(\boldsymbol{\tau}_h, \boldsymbol{\tau}_h) \leq \alpha_2 (\|\boldsymbol{\tau}_h\|_{0,E}^2 + \|\boldsymbol{\tau}_h - \Pi_h^E \boldsymbol{\tau}_h\|_{0,E}^2) \quad \forall \boldsymbol{\tau}_h \in \mathbb{H}_h^E.$$

Proof. See [11, Lemma 4.6]. □

Now, for bilinear form $b(\cdot, \cdot)$ we have

$$b(\boldsymbol{\tau}_h, \mathbf{v}_h) = \sum_{E \in \mathcal{T}_h} b^E(\boldsymbol{\tau}_h, \mathbf{v}_h) = \sum_{E \in \mathcal{T}_h} \int_E \mathbf{v}_h \cdot \operatorname{div} \boldsymbol{\tau}_h,$$

which is explicitly computable with the degrees of freedom of $\mathbb{H}_{0,h}$ and \mathbf{Q}_h .

With these bilinear forms at hand, we introduce the VEM discretization of (2.2): find $\kappa_h \in \mathbb{R}^+$ and $(\boldsymbol{\rho}_h, \mathbf{u}_h) \in \mathbb{H}_{0,h} \times \mathbf{Q}_h$ such that

$$(3.4) \quad \begin{cases} a_h(\boldsymbol{\rho}_h, \boldsymbol{\tau}_h) + b(\boldsymbol{\tau}_h, \mathbf{u}_h) &= 0 & \forall \boldsymbol{\tau}_h \in \mathbb{H}_{0,h}, \\ b(\boldsymbol{\rho}_h, \mathbf{v}_h) &= -\kappa_h c_h(\mathbf{u}_h, \mathbf{v}_h) & \forall \mathbf{v}_h \in \mathbf{Q}_h. \end{cases}$$

Now we introduce the discrete solution operators as follows

$$\mathbf{T}_h : \mathbf{Q} \rightarrow \mathbf{Q}_h, \quad \mathbf{f} \mapsto \mathbf{T}_h \mathbf{f} := \widehat{\mathbf{u}}_h, \quad \mathcal{S} : \mathbf{Q} \rightarrow \mathbb{H}_{0,h}, \quad \mathbf{f} \mapsto \mathcal{S}_h \mathbf{f} := \widehat{\boldsymbol{\rho}}_h$$

where the pair $(\widehat{\boldsymbol{\rho}}_h, \widehat{\mathbf{u}}_h) \in \mathbb{H}_{0,h} \times \mathbf{Q}_h$ is the solution of the following source problem

$$(3.5) \quad \begin{cases} a_h(\widehat{\boldsymbol{\rho}}_h, \boldsymbol{\tau}_h) + b(\boldsymbol{\tau}_h, \widehat{\mathbf{u}}_h) &= 0 & \forall \boldsymbol{\tau}_h \in \mathbb{H}_{0,h}, \\ b(\widehat{\boldsymbol{\rho}}_h, \mathbf{v}_h) &= -c_h(\mathbf{f}, \mathbf{v}_h) & \forall \mathbf{v}_h \in \mathbf{Q}_h. \end{cases}$$

The discrete kernel of $b(\cdot, \cdot)$ is defined by $\mathbb{V}_h := \{\boldsymbol{\tau}_h \in \mathbb{H}_{0,h} : b(\boldsymbol{\tau}_h, \mathbf{v}_h) = 0 \quad \forall \mathbf{v}_h \in \mathbf{Q}_h\} \subset \mathbb{V}$. Hence, invoking Lemma 3.1 it is direct to prove that $a_h(\cdot, \cdot)$ is \mathbb{V}_h -coercive. More precisely, there exists a positive constant $\widehat{\alpha}$, independent of h and λ , such that

$$a_h(\boldsymbol{\tau}_h, \boldsymbol{\tau}_h) \geq \widehat{\alpha} \|\boldsymbol{\tau}_h\|_{\operatorname{div}, \Omega}.$$

Moreover, the following inf-sup condition is satisfied (see [15, Lemma 3.1])

$$(3.6) \quad \sup_{\mathbf{0} \neq \boldsymbol{\tau}_h \in \mathbb{H}_{0,h}} \frac{b(\boldsymbol{\tau}_h, \mathbf{v}_h)}{\|\boldsymbol{\tau}_h\|_{\operatorname{div}, \Omega}} \geq \widetilde{\beta} \|\mathbf{v}\|_{0, \Omega},$$

with $\tilde{\beta} > 0$ independent of h . By the previous results, together with the Babuška-Brezzi theory, the discrete operators \mathbf{T}_h and \mathbf{S}_h are well defined.

We collect here the approximation properties required in the next section. Let $\mathcal{I}_k^h : \mathbb{H}^t(\Omega) \rightarrow \mathbb{W}_h$ be the tensorial version of the VEM-interpolation operator. For $t > 1/2$, it holds (see [6, Lemma 6])

$$\|\boldsymbol{\tau} - \mathcal{I}_k^h \boldsymbol{\tau}\|_{0,\Omega} \leq Ch^{\min\{t,k+1\}} \|\boldsymbol{\tau}\|_{t,\Omega} \quad \forall \boldsymbol{\tau} \in \mathbb{H}^t(\Omega).$$

For $\boldsymbol{\tau} \in \mathbb{H}^t(\Omega) \cap \mathbb{H}(\operatorname{div}; \Omega)$ with $t \in (0, 1/2]$, one has the estimate, see [18, Theorem 3.16]

$$\|\boldsymbol{\tau} - \mathcal{I}_k^h \boldsymbol{\tau}\|_{0,\Omega} \leq Ch^t (\|\boldsymbol{\tau}\|_{t,\Omega} + \|\boldsymbol{\tau}\|_{\operatorname{div},\Omega}).$$

Moreover, \mathcal{I}_k^h satisfies the commuting diagram property (see [6, Lemma 5]):

$$\|\operatorname{div}(\boldsymbol{\tau} - \mathcal{I}_k^h \boldsymbol{\tau})\|_{0,\Omega} = \|\operatorname{div} \boldsymbol{\tau} - \mathcal{P}_k^h \operatorname{div} \boldsymbol{\tau}\|_{0,\Omega} \leq Ch^{\min\{t,k\}} \|\operatorname{div} \boldsymbol{\tau}\|_{t,\Omega},$$

for $\operatorname{div} \boldsymbol{\tau} \in \mathbb{H}^t(\Omega)^2$ where \mathcal{P}_k^h denotes the L^2 -orthogonal projection onto \mathbb{P}_k . Finally, we set $\boldsymbol{\tau}_I := \mathcal{I}_k^h(\boldsymbol{\tau})|_E \in \mathbb{H}_h^E$.

Finally, as we did on the continuous setting, for all $\boldsymbol{\rho}_h, \boldsymbol{\tau}_h \in \widehat{\mathbb{H}}_{0,h}$ and for all $\mathbf{v}_h, \mathbf{u}_h \in \mathbf{Q}_h$, we define the following discrete bilinear form

$$A_h((\boldsymbol{\rho}_h, \mathbf{u}_h), (\boldsymbol{\tau}_h, \mathbf{v}_h)) := a_h(\boldsymbol{\rho}_h, \boldsymbol{\tau}_h) + b(\boldsymbol{\tau}_h, \mathbf{u}_h) + b(\boldsymbol{\rho}_h, \mathbf{v}_h).$$

4. Spectral convergence. We begin this section by proving that the discrete solution operator \mathbf{T}_h converges to \mathbf{T} as $h \rightarrow 0$. This is contained in the following result.

THEOREM 4.1. *Let $\mathbf{f} \in \mathbf{Q}$ be such that $\widehat{\mathbf{u}} := \mathbf{T}\mathbf{f}$, $\widehat{\boldsymbol{\rho}} := \mathbf{S}\mathbf{f}$ and $\widehat{\mathbf{u}}_h := \mathbf{T}\mathbf{f}$, $\widehat{\boldsymbol{\rho}}_h := \mathbf{S}_h\mathbf{f}$, where $(\widehat{\boldsymbol{\rho}}, \widehat{\mathbf{u}}) \in \mathbb{H}_0 \times \mathbf{Q}$ is the solution of (2.4) and $(\widehat{\boldsymbol{\rho}}_h, \widehat{\mathbf{u}}_h) \in \widehat{\mathbb{H}}_{0,h} \times \mathbf{Q}_h$ is the solution of (3.5). Then, there holds where the hidden constant is independent of h and s is the regularity exponent provided by Lemma 2.1.*

Proof. Let $\widehat{\mathbf{u}}_I$ and $\mathcal{I}_k^h \widehat{\boldsymbol{\rho}}$ be the best approximations of $\widehat{\mathbf{u}}$ and $\widehat{\boldsymbol{\rho}}$, respectively. Hence, from the definitions of the solution operators, elementary calculations lead to

$$(4.1) \quad \|(\mathbf{T} - \mathbf{T}_h)\mathbf{f}\|_{0,\Omega} = \|\widehat{\mathbf{u}} - \widehat{\mathbf{u}}_I\|_{0,\Omega} \leq \underbrace{\|\widehat{\mathbf{u}} - \mathcal{P}_k^h(\widehat{\mathbf{u}})\|_{0,\Omega}}_{\text{I}} + \underbrace{\|\mathcal{P}_k^h(\widehat{\mathbf{u}}) - \widehat{\mathbf{u}}\|_{0,\Omega}}_{\text{II}}$$

where the task is to estimate terms I and II. For I, using the regularity of $\widehat{\mathbf{u}}$ and the dependency on the data \mathbf{f} , we have

$$(4.2) \quad \text{I} \leq Ch^s \|\mathbf{f}\|_{0,\Omega}.$$

Now for the term II, we taking $\mathbf{v}_h := \mathcal{P}_k(\widehat{\mathbf{u}}) - \widehat{\mathbf{u}} \in \mathbf{Q}_h$ in the discrete inf-sup condition (3.6), we obtain

$$\|\mathcal{P}_k^h(\widehat{\mathbf{u}}) - \widehat{\mathbf{u}}\|_{0,\Omega} \leq \frac{1}{\tilde{\beta}} \sup_{\mathbf{0} \neq \boldsymbol{\tau}_h \in \widehat{\mathbb{H}}_{0,h}} \frac{b(\boldsymbol{\tau}_h, \mathcal{P}_k^h(\widehat{\mathbf{u}}) - \widehat{\mathbf{u}})}{\|\boldsymbol{\tau}_h\|_{\operatorname{div},\Omega}}.$$

Now, since $\boldsymbol{\tau}_h \in \widehat{\mathbb{H}}_{0,h}$, we have that $\operatorname{div} \boldsymbol{\tau}_h \in \mathbf{Q}_h$. Then, recalling that \mathcal{P}_k is the

L^2 -orthogonal projection, we obtain

$$\begin{aligned}
b(\boldsymbol{\tau}_h, \mathcal{P}_k^h(\widehat{\mathbf{u}}) - \widehat{\mathbf{u}}) &= b(\boldsymbol{\tau}_h, \mathcal{P}_k^h(\widehat{\mathbf{u}})) - b(\boldsymbol{\tau}_h, \widehat{\mathbf{u}}) = b(\boldsymbol{\tau}_h, \widehat{\mathbf{u}}) - b(\boldsymbol{\tau}_h, \widehat{\mathbf{u}}) \\
&= a_h(\widehat{\boldsymbol{\rho}}_h, \boldsymbol{\tau}_h) - a(\widehat{\boldsymbol{\rho}}, \boldsymbol{\tau}_h) = a_h(\widehat{\boldsymbol{\rho}}_h - \mathcal{I}_k^h \widehat{\boldsymbol{\rho}}, \boldsymbol{\tau}_h) + a_h(\mathcal{I}_k^h \widehat{\boldsymbol{\rho}}, \boldsymbol{\tau}_h) - a(\widehat{\boldsymbol{\rho}}, \boldsymbol{\tau}_h) \\
&= a_h(\widehat{\boldsymbol{\rho}}_h - \mathcal{I}_k^h \widehat{\boldsymbol{\rho}}, \boldsymbol{\tau}_h) + \sum_{E \in \mathcal{T}_h} [a_h^E(\mathcal{I}_k^h \widehat{\boldsymbol{\rho}} - \Pi_h^E \widehat{\boldsymbol{\rho}}, \boldsymbol{\tau}_h) + a^E(\Pi_h^E \widehat{\boldsymbol{\rho}} - \widehat{\boldsymbol{\rho}}, \boldsymbol{\tau}_h)] \\
&\leq C \left(\|\widehat{\boldsymbol{\rho}}_h - \mathcal{I}_k^h \widehat{\boldsymbol{\rho}}\|_{0,\Omega} \|\boldsymbol{\tau}_h\|_{0,\Omega} \right. \\
&\quad \left. + \sum_{E \in \mathcal{T}_h} \left(\|\widehat{\boldsymbol{\rho}} - \mathcal{I}_k^h \widehat{\boldsymbol{\rho}}\|_{0,E} + 2\|\widehat{\boldsymbol{\rho}} - \Pi_h^E \widehat{\boldsymbol{\rho}}\|_{0,E} \right) \|\boldsymbol{\tau}_h\|_{0,E} \right).
\end{aligned}$$

Thanks to the previous estimate, we conclude that:

$$(4.3) \quad \|\mathcal{P}_k^h(\widehat{\mathbf{u}}) - \widehat{\mathbf{u}}\|_{0,\Omega} \leq \frac{C}{\beta} \left(\|\widehat{\boldsymbol{\rho}}_h - \mathcal{I}_k^h \widehat{\boldsymbol{\rho}}\|_{0,\Omega} + \sum_{E \in \mathcal{T}_h} \left(\|\widehat{\boldsymbol{\rho}} - \mathcal{I}_k^h \widehat{\boldsymbol{\rho}}\|_{0,E} + 2\|\widehat{\boldsymbol{\rho}} - \Pi_h^E \widehat{\boldsymbol{\rho}}\|_{0,E} \right) \right).$$

The following step consists in bounding the first term of the previous estimate. To this purpose, the commutative diagram property reveals

$$\operatorname{div} \mathcal{I}_k^h \widehat{\boldsymbol{\rho}} = \mathcal{P}_k^h(\operatorname{div} \boldsymbol{\rho}) = -\mathcal{P}_k^h(\mathbf{f}) = \operatorname{div} \widehat{\boldsymbol{\rho}}_h,$$

and as a result, $\mathcal{I}_k^h \widehat{\boldsymbol{\rho}} - \widehat{\boldsymbol{\rho}}_h \in \mathbb{V}_h$. Now, by defining $\boldsymbol{\varphi} = \widehat{\boldsymbol{\rho}}_h - \mathcal{I}_k^h \widehat{\boldsymbol{\rho}}$ we have

$$\begin{aligned}
C \|\widehat{\boldsymbol{\rho}}_h - \mathcal{I}_k^h \widehat{\boldsymbol{\rho}}\|_{\operatorname{div},\Omega}^2 &= C \|\widehat{\boldsymbol{\rho}}_h - \mathcal{I}_k^h \widehat{\boldsymbol{\rho}}\|_{0,\Omega}^2 \leq a_h(\widehat{\boldsymbol{\rho}}_h - \mathcal{I}_k^h \widehat{\boldsymbol{\rho}}, \boldsymbol{\varphi}) = a_h(\widehat{\boldsymbol{\rho}}_h, \boldsymbol{\varphi}) - a_h(\mathcal{I}_k^h \widehat{\boldsymbol{\rho}}, \boldsymbol{\varphi}) \\
&= -b(\boldsymbol{\varphi}, \widehat{\mathbf{u}}_h) - a_h(\mathcal{I}_k^h \widehat{\boldsymbol{\rho}}, \boldsymbol{\varphi}) = -a_h(\mathcal{I}_k^h \widehat{\boldsymbol{\rho}}, \boldsymbol{\varphi}) \\
&= - \sum_{E \in \mathcal{T}_h} [a_h^E(\mathcal{I}_k^h \widehat{\boldsymbol{\rho}} - \Pi_h^E \widehat{\boldsymbol{\rho}}, \boldsymbol{\tau}_h) + a^E(\Pi_h^E \widehat{\boldsymbol{\rho}} - \widehat{\boldsymbol{\rho}}, \boldsymbol{\tau}_h) + a^E(\widehat{\boldsymbol{\rho}}, \boldsymbol{\tau}_h)] \\
&= \sum_{E \in \mathcal{T}_h} [a_h^E(\Pi_h^E \widehat{\boldsymbol{\rho}} - \mathcal{I}_k^h \widehat{\boldsymbol{\rho}}, \boldsymbol{\tau}_h) + a^E(\widehat{\boldsymbol{\rho}} - \Pi_h^E \widehat{\boldsymbol{\rho}}, \boldsymbol{\tau}_h)] \\
&\leq C \sum_{E \in \mathcal{T}_h} \left(\|\widehat{\boldsymbol{\rho}} - \mathcal{I}_k^h \widehat{\boldsymbol{\rho}}\|_{0,\Omega} + 2\|\widehat{\boldsymbol{\rho}} - \Pi_h^E \widehat{\boldsymbol{\rho}}\|_{0,\Omega} \right) \|\boldsymbol{\varphi}_h\|_{0,\Omega}.
\end{aligned}$$

Then

$$\|\widehat{\boldsymbol{\rho}}_h - \mathcal{I}_k^h \widehat{\boldsymbol{\rho}}\|_{0,\Omega} \leq C \sum_{E \in \mathcal{T}_h} \left(\|\widehat{\boldsymbol{\rho}} - \mathcal{I}_k^h \widehat{\boldsymbol{\rho}}\|_{0,\Omega} + 2\|\widehat{\boldsymbol{\rho}} - \Pi_h^E \widehat{\boldsymbol{\rho}}\|_{0,\Omega} \right).$$

Replacing the previous estimate in (4.3), we arrive to

$$(4.4) \quad \|\mathcal{P}_k^h(\widehat{\mathbf{u}}) - \widehat{\mathbf{u}}\|_{0,\Omega} \leq \frac{C}{\beta} \left(\sum_{E \in \mathcal{T}_h} \left(2\|\widehat{\boldsymbol{\rho}} - \mathcal{I}_k^h \widehat{\boldsymbol{\rho}}\|_{0,E} + 4\|\widehat{\boldsymbol{\rho}} - \Pi_h^E \widehat{\boldsymbol{\rho}}\|_{0,E} \right) \right) \leq \frac{C}{\beta} h^s \|\mathbf{f}\|_{0,\Omega}.$$

Thus, combining (4.1), (4.2), and (4.4), the proof is complete. \square

With Theorem 4.1 at hand, and invoking the well established theory of [20, Chapter IV] and [7, Theorem 9.1], we are in position to conclude that our numerical methods do not introduce spurious eigenvalues. This is stated in the following theorem.

THEOREM 4.2. *Let $V \subset \mathbb{C}$ be an open set containing $\operatorname{sp}(\mathbf{T})$. Then, there exists $h_0 > 0$ such that $\operatorname{sp}(\mathbf{T}_h) \subset V$ for all $h < h_0$.*

We end this section providing an improvement for the L^2 order of the displacement.

LEMMA 4.3. *There exists a constant $C > 0$, independent of h , such that*

$$\|\mathbf{u} - \mathbf{u}_h\|_{0,\Omega} \leq Ch^{2s}.$$

Proof. We use a standard duality argument. Let us consider the following auxiliary problem: Find $(\boldsymbol{\varphi}, \boldsymbol{\psi}) \in \mathbb{H}_0 \times \mathbf{Q}$ such that

$$(4.5) \quad \begin{cases} a(\boldsymbol{\varphi}, \boldsymbol{\tau}) + b(\boldsymbol{\tau}, \boldsymbol{\psi}) &= 0 & \forall \boldsymbol{\tau} \in \mathbb{H}_0, \\ b(\boldsymbol{\varphi}, \mathbf{v}) &= -c(\widehat{\mathbf{u}} - \widehat{\mathbf{u}}_h, \mathbf{v}) & \forall \mathbf{v} \in \mathbf{Q}. \end{cases}$$

In this case the solution satisfies:

$$\|\boldsymbol{\varphi}\|_{s,\Omega} + \|\mathbf{div} \boldsymbol{\varphi}\|_{1+s,\Omega} + \|\boldsymbol{\psi}\|_{1+s} \leq C\|\widehat{\mathbf{u}} - \widehat{\mathbf{u}}_h\|_{0,\Omega}.$$

Let $\mathcal{I}_k^h \boldsymbol{\varphi} \in \mathbb{H}_h$, be the virtual interpolator of $\boldsymbol{\varphi}$. Adding and subtracting $\mathcal{I}_k^h \boldsymbol{\varphi}$ and testing (4.5) with $\mathbf{v} = \widehat{\mathbf{u}} - \widehat{\mathbf{u}}_h$ yield to

$$(4.6) \quad \|\widehat{\mathbf{u}} - \widehat{\mathbf{u}}_h\|_{0,\Omega}^2 = b(\boldsymbol{\varphi} - \mathcal{I}_k^h \boldsymbol{\varphi}, \widehat{\mathbf{u}}_h - \widehat{\mathbf{u}}) + b(\mathcal{I}_k^h \boldsymbol{\varphi}, \widehat{\mathbf{u}}_h - \widehat{\mathbf{u}}).$$

Using the continuous and discrete source problems (2.4) and (3.5), respectively, testing with discrete functions in (2.4), and subtracting the first equation on these problems, we obtain the following identity

$$a(\widehat{\boldsymbol{\rho}}, \boldsymbol{\tau}_h) - a_h(\widehat{\boldsymbol{\rho}}, \boldsymbol{\tau}_h) = b(\boldsymbol{\tau}_h, \widehat{\mathbf{u}}_h - \widehat{\mathbf{u}}) \quad \forall \boldsymbol{\tau}_h \in \mathbb{H}_{0,h},$$

whereas if we consider the second equation on each source problem, where the continuous one is tested with $\mathbf{v}_h \in \mathbf{Q}_h$, we obtain after the subtraction the following equation

$$(4.7) \quad b(\widehat{\boldsymbol{\rho}} - \widehat{\boldsymbol{\rho}}_h, \mathbf{v}_h) = 0 \quad \forall \mathbf{v}_h \in \mathbf{Q}_h.$$

Now, from (4.6) we obtain the following identity

$$\begin{aligned} \|\widehat{\mathbf{u}} - \widehat{\mathbf{u}}_h\|_{0,\Omega}^2 &= b(\boldsymbol{\varphi} - \mathcal{I}_k^h \boldsymbol{\varphi}, \widehat{\mathbf{u}}_h - \widehat{\mathbf{u}}) + a(\widehat{\boldsymbol{\rho}}, \mathcal{I}_k^h \boldsymbol{\varphi}) - a_h(\widehat{\boldsymbol{\rho}}_h, \mathcal{I}_k^h \boldsymbol{\varphi}) \\ &= \underbrace{b(\boldsymbol{\varphi} - \mathcal{I}_k^h \boldsymbol{\varphi}, \widehat{\mathbf{u}}_h - \widehat{\mathbf{u}})}_{T_1} + \underbrace{a(\widehat{\boldsymbol{\rho}} - \widehat{\boldsymbol{\rho}}_h, \mathcal{I}_k^h \boldsymbol{\varphi})}_{T_2} + \underbrace{a(\widehat{\boldsymbol{\rho}}_h, \mathcal{I}_k^h \boldsymbol{\varphi}) - a_h(\widehat{\boldsymbol{\rho}}_h, \mathcal{I}_k^h \boldsymbol{\varphi})}_{T_3}, \end{aligned}$$

where the task now is to estimate the terms T_1 , T_2 , and T_3 . For T_2 we have

$$\begin{aligned} T_2 &= a(\widehat{\boldsymbol{\rho}} - \widehat{\boldsymbol{\rho}}_h, \mathcal{I}_k^h \boldsymbol{\varphi} - \boldsymbol{\varphi}) + a(\widehat{\boldsymbol{\rho}} - \widehat{\boldsymbol{\rho}}_h, \boldsymbol{\varphi}) \\ &= a(\widehat{\boldsymbol{\rho}} - \widehat{\boldsymbol{\rho}}_h, \mathcal{I}_k^h \boldsymbol{\varphi} - \boldsymbol{\varphi}) + a(\boldsymbol{\varphi}, \widehat{\boldsymbol{\rho}} - \widehat{\boldsymbol{\rho}}_h) \\ &= a(\widehat{\boldsymbol{\rho}} - \widehat{\boldsymbol{\rho}}_h, \mathcal{I}_k^h \boldsymbol{\varphi} - \boldsymbol{\varphi}) - b(\widehat{\boldsymbol{\rho}} - \widehat{\boldsymbol{\rho}}_h, \boldsymbol{\psi}) \\ &= a(\widehat{\boldsymbol{\rho}} - \widehat{\boldsymbol{\rho}}_h, \mathcal{I}_k^h \boldsymbol{\varphi} - \boldsymbol{\varphi}) - b(\widehat{\boldsymbol{\rho}} - \widehat{\boldsymbol{\rho}}_h, \boldsymbol{\psi} - \mathcal{P}_k(\boldsymbol{\psi})) - b(\widehat{\boldsymbol{\rho}} - \widehat{\boldsymbol{\rho}}_h, \mathcal{P}_k(\boldsymbol{\psi})) \\ &= a(\widehat{\boldsymbol{\rho}} - \widehat{\boldsymbol{\rho}}_h, \mathcal{I}_k^h \boldsymbol{\varphi} - \boldsymbol{\varphi}) - b(\widehat{\boldsymbol{\rho}} - \widehat{\boldsymbol{\rho}}_h, \boldsymbol{\psi} - \mathcal{P}_k(\boldsymbol{\psi})), \end{aligned}$$

where for the last equality we have used (4.7). For T_3 , we have to operate element

by element as follows

$$\begin{aligned}
T_3 &= \sum_{E \in \mathcal{T}_h} \left(a^E(\widehat{\rho}_h, \mathcal{I}_k^h \varphi) - a_h^E(\widehat{\rho}_h, \mathcal{I}_k^h \varphi) \right) \\
&= \sum_{E \in \mathcal{T}_h} \left(a^E(\widehat{\rho}_h - \Pi_h^E \widehat{\rho}, \mathcal{I}_k^h \varphi) - a_h^E(\widehat{\rho}_h - \Pi_h^E \widehat{\rho}, \mathcal{I}_k^h \varphi) \right) \\
&= \sum_{E \in \mathcal{T}_h} \left(a^E(\widehat{\rho}_h - \Pi_h^E \widehat{\rho}, \mathcal{I}_k^h \varphi - \Pi_h^E \varphi_\pi) - a_h^E(\widehat{\rho}_h - \Pi_h^E \widehat{\rho}, \mathcal{I}_k^h \varphi - \Pi_h^E \varphi_\pi) \right).
\end{aligned}$$

In the previous equality, we have used that $\Pi_h^E \widehat{\rho} \in \mathbb{L}^2(\Omega)$ and satisfies that $\widehat{\rho}_\psi|_E \in \mathcal{P}_k(E)$ for all $E \in \mathcal{T}_h$ and the same satisfies the term $\Pi_h^E \varphi_\pi$. Now, combining all the estimates, we obtain that

$$\begin{aligned}
\|\widehat{\mathbf{u}} - \widehat{\mathbf{u}}_h\|_{0,\Omega}^2 &= b(\varphi - \mathcal{I}_k^h \varphi, \widehat{\mathbf{u}}_h - \widehat{\mathbf{u}}) + a(\widehat{\rho} - \widehat{\rho}_h, \mathcal{I}_k^h \varphi - \varphi) - b(\widehat{\rho} - \widehat{\rho}_h, \psi - \mathcal{P}_k(\psi)) \\
&\quad + \sum_{E \in \mathcal{T}_h} \left(a^E(\widehat{\rho}_h - \Pi_h^E \widehat{\rho}, \mathcal{I}_k^h \varphi - \Pi_h^E \varphi_\pi) - a_h^E(\widehat{\rho}_h - \Pi_h^E \widehat{\rho}, \mathcal{I}_k^h \varphi - \Pi_h^E \varphi_\pi) \right) \\
&\leq C \left(\|\mathbf{div}(\varphi - \mathcal{I}_k^h \varphi)\|_{0,\Omega} \|\widehat{\mathbf{u}} - \widehat{\mathbf{u}}_h\|_{0,\Omega} + \|\widehat{\rho} - \widehat{\rho}_h\|_{0,\Omega} \|\varphi - \mathcal{I}_k^h \varphi\|_{0,\Omega} \right. \\
&\quad \left. + \|\mathbf{div}(\widehat{\rho} - \widehat{\rho}_h)\|_{0,\Omega} \|\psi - \mathcal{P}_k(\psi)\|_{0,\Omega} \right) \\
&\quad + 2 \sum_{E \in \mathcal{T}_h} \left(\|\widehat{\rho} - \widehat{\rho}_h\|_{0,E} + \|\widehat{\rho} - \Pi_h^E \widehat{\rho}\|_{0,E} \right) \left(\|\varphi - \mathcal{I}_k^h \varphi\|_{0,E} + \|\varphi - \Pi_h^E \varphi_\pi\|_{0,E} \right) \\
&\leq Ch^{2s} \|\widehat{\mathbf{u}} - \widehat{\mathbf{u}}_h\|_{0,\Omega}.
\end{aligned}$$

This concludes the proof. \square

4.1. Error estimates. We first recall the definition of spectral projectors. Let η be a nonzero isolated eigenvalue of \mathbf{T} with algebraic multiplicity m and let Γ be a disk of the complex plane centered in η , such that η is the only eigenvalue of \mathbf{T} lying in Γ and $\partial\Gamma \cap \text{sp}(\mathbf{T}) = \emptyset$. With these considerations at hand, we define the spectral projection of \mathbf{E} associated to \mathbf{T} as follows:

- The spectral projector of \mathbf{T} associated to η is $\mathbf{E} := \frac{1}{2\pi i} \int_{\partial\Gamma} (z\mathbf{I} - \mathbf{T})^{-1} dz$;

where \mathbf{I} represents the identity operator. Let us remark that \mathbf{E} is the projection onto the generalized eigenspace $R(\mathbf{E})$. A consequence of Theorem 4.1 is that there exist m eigenvalues, which lie in Γ , namely $\eta_{h,1}, \dots, \eta_{h,m}$, repeated according their respective multiplicities, that converge to η as h goes to zero. With this result at hand, we introduce the following spectral projection

$$\mathbf{E}_h := \frac{1}{2\pi i} \int_{\partial\Gamma} (z\mathbf{I} - \mathbf{T}_h)^{-1} dz,$$

which is a projection onto the discrete invariant subspace $R(\mathbf{E}_h)$ of \mathbf{T} , spanned by the generalized eigenvector of \mathbf{T}_h corresponding to $\eta_{h,1}, \dots, \eta_{h,m}$.

Now we recall the definition of the gap $\widehat{\delta}(\cdot, \cdot)$ between two closed subspaces \mathfrak{X} and \mathfrak{Y} of $\mathbf{L}^2(\Omega)$:

$$\widehat{\delta}(\mathfrak{X}, \mathfrak{Y}) := \max \{ \delta(\mathfrak{X}, \mathfrak{Y}), \delta(\mathfrak{Y}, \mathfrak{X}) \}, \text{ where } \delta(\mathfrak{X}, \mathfrak{Y}) := \sup_{\substack{\mathbf{x} \in \mathfrak{X} \\ \|\mathbf{x}\|_{0,\Omega}=1}} \left(\inf_{\mathbf{y} \in \mathfrak{Y}} \|\mathbf{x} - \mathbf{y}\|_{0,\Omega} \right).$$

With these definitions at hand, we derive the following error estimates for eigenfunctions and eigenvalues by following the results from [7, Theorems 13.8 and 13.10].

THEOREM 4.4. *The following estimates hold*

$$\widehat{\delta}(R(\mathbf{E}), R(\mathbf{E}_h)) \leq Ch^{\min\{r, k+1\}} \quad \text{and} \quad |\eta - \eta_{h,i}| \leq Ch^{\min\{r, k+1\}}. \quad i = 1, \dots, m,$$

where the regularity parameter $r > 0$ is the same as in Lemma 2.1 and the constant $C > 0$ is independent of λ and h .

The following theorem establishes the double order of convergence for the eigenvalues. To this end, we note that the error estimate for the eigenvalue μ of \mathbf{T} leads to an analogous estimate for the approximation of the eigenvalue $\kappa = \frac{1}{\eta}$ of (2.2) with eigenspace \mathcal{E} . Let $\kappa_{h,i} = \frac{1}{\eta_{h,i}}$, $1 \leq i \leq m$ be the eigenvalues of (3.4) with invariant subspace \mathcal{E}_h . Therefore we have the following result.

THEOREM 4.5. *There exist positive constants C , independent of λ , and h_0 , such that for $h < h_0$*

$$|\kappa - \kappa_{h,i}| \leq Ch^{2\min\{r, k+1\}}, \quad i = 1, \dots, m.$$

Proof. Let $\mathbf{u}_h \in \mathcal{E}_h$ be an eigenfunction associated to the eigenvalue $\kappa_h^{(i)}$, with $i = 1, \dots, m$, such that $c_h(\mathbf{u}_h, \mathbf{u}_h) = \|\mathbf{u}_h\|_{0,\Omega}^2 = 1$. Consider the following eigenvalue problems

$$A((\boldsymbol{\rho}, \mathbf{u}), (\boldsymbol{\rho}, \mathbf{u})) = -\kappa c(\mathbf{u}, \mathbf{u}) \quad \forall (\boldsymbol{\rho}, \mathbf{u}) \in \mathbb{H}_0 \times \mathbf{Q},$$

and

$$A_h((\boldsymbol{\rho}_h, \mathbf{u}_h), (\boldsymbol{\rho}_h, \mathbf{u}_h)) = -\kappa_{h,i} c_h(\mathbf{u}_h, \mathbf{u}_h) \quad \forall (\boldsymbol{\rho}_h, \mathbf{u}_h) \in \mathbb{H}_{0,h} \times \mathbf{Q}_h.$$

With these problems at hand, the following identity is straightforward

$$(4.8) \quad (\kappa - \kappa_h^{(i)})c(\mathbf{u}_h, \mathbf{u}_h) = \underbrace{A((\boldsymbol{\rho}_h - \boldsymbol{\rho}_h, \mathbf{u} - \mathbf{u}_h), (\boldsymbol{\rho}_h - \boldsymbol{\rho}_h, \mathbf{u} - \mathbf{u}_h))}_{\Lambda_1} + \underbrace{\kappa c(\mathbf{u} - \mathbf{u}_h, \mathbf{u} - \mathbf{u}_h)}_{\Lambda_2} + \underbrace{\sum_{E \in \mathcal{T}_h} a_h^E(\boldsymbol{\rho}_h, \boldsymbol{\rho}_h) - a^E(\boldsymbol{\rho}_h, \boldsymbol{\rho}_h)}_{\Lambda_3}.$$

The task is to control each contribution on the right-hand side of (4.8). Let us begin with Λ_1 . Using the definition of $A(\cdot, \cdot)$, triangle inequality, Cauchy-Schwarz inequality, the fact that $1/(4\lambda + 6\mu) < 1/6\mu$ and the regularity of the eigenfunctions,

we have

$$\begin{aligned}
(4.9) \quad |\Lambda_1| &\leq |a(\boldsymbol{\rho} - \boldsymbol{\rho}_h, \boldsymbol{\rho} - \boldsymbol{\rho}_h)| + 2|b(\boldsymbol{\rho} - \boldsymbol{\rho}_h, \mathbf{u} - \mathbf{u}_h)| \\
&\leq \frac{1}{\mu} \|(\boldsymbol{\rho} - \boldsymbol{\rho}_h)^d\|_{0,\Omega}^2 + \frac{1}{4\lambda + 6\mu} \|\operatorname{tr}(\boldsymbol{\rho} - \boldsymbol{\rho}_h)\|_{0,\Omega}^2 + 2\|\mathbf{div}(\boldsymbol{\rho} - \boldsymbol{\rho}_h)\|_{0,\Omega} \|\mathbf{u} - \mathbf{u}_h\|_{0,\Omega} \\
&\leq \frac{3(2 + \sqrt{2})^2 + 2}{12\mu} \|(\boldsymbol{\rho} - \boldsymbol{\rho}_h)\|_{0,\Omega}^2 + \|\mathbf{div}(\boldsymbol{\rho} - \boldsymbol{\rho}_h)\|_{0,\Omega}^2 + \|\mathbf{u} - \mathbf{u}_h\|_{0,\Omega}^2 \\
&\leq \max \left\{ \frac{3(2 + \sqrt{2})^2 + 2}{12\mu}, 1 \right\} (\|\boldsymbol{\rho} - \boldsymbol{\rho}_h\|_{\mathbf{div},\Omega}^2 + \|\mathbf{u} - \mathbf{u}_h\|_{0,\Omega}^2) \\
&\leq C \max \left\{ \frac{3(2 + \sqrt{2})^2 + 2}{12\mu}, 1 \right\} h^{2\min\{r,k+1\}}.
\end{aligned}$$

The control of Λ_2 is straightforward:

$$(4.10) \quad \Lambda_2 \leq \|\mathbf{u} - \mathbf{u}_h\|_{0,\Omega}^2 \leq Ch^{2\min\{r,k+1\}}$$

Now, for Λ_3 we invoke the consistency in order to obtain the following estimate

$$\begin{aligned}
(4.11) \quad |\Lambda_3| &= \left| \sum_{E \in \mathcal{T}_h} a_h^E(\boldsymbol{\rho}_h, \boldsymbol{\rho}_h) - a^E(\boldsymbol{\rho}_h, \boldsymbol{\rho}_h) \right| \\
&= \left| \sum_{E \in \mathcal{T}_h} a_h^E(\boldsymbol{\rho}_h - \Pi_h^E \boldsymbol{\rho}, \boldsymbol{\rho}_h) - a^E(\boldsymbol{\rho}_h - \Pi_h^E \boldsymbol{\rho}, \boldsymbol{\rho}_h) \right| \\
&= \left| \sum_{E \in \mathcal{T}_h} a_h^E(\boldsymbol{\rho}_h - \Pi_h^E \boldsymbol{\rho}, \boldsymbol{\rho}_h - \Pi_h^E \boldsymbol{\rho}) - a^E(\boldsymbol{\rho}_h - \Pi_h^E \boldsymbol{\rho}, \boldsymbol{\rho}_h - \Pi_h^E \boldsymbol{\rho}) \right| \\
&\leq \sum_{E \in \mathcal{T}_h} \|\boldsymbol{\rho}_h - \Pi_h^E \boldsymbol{\rho}\|_{0,E}^2 \leq \sum_{E \in \mathcal{T}_h} \|\boldsymbol{\rho}_h - \boldsymbol{\rho}\|_{0,E}^2 + \|\Pi_h^E \boldsymbol{\rho} - \boldsymbol{\rho}\|_{0,E}^2 \leq Ch^{2\min\{r,k+1\}}.
\end{aligned}$$

Hence, gathering (4.9), (4.10) and (4.11), and replacing all these estimates in (4.8), we conclude the proof. \square

5. Numerical experiments. This section is devoted to perform several numerical experiments to analyze the behavior of the scheme in different geometries and physical configurations. We have performed the computational tests with a MATLAB code, using different meshes like the ones presented in Figure 1. The eigenvalue problem is solved with the command `eigs`.

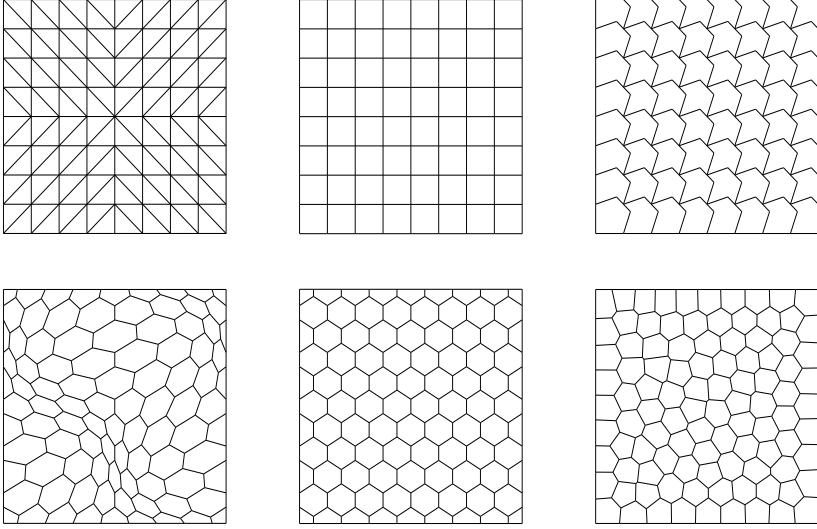


FIG. 1. Sample meshes: \mathcal{T}_h^1 (top left), \mathcal{T}_h^2 (top middle), \mathcal{T}_h^3 (top right), \mathcal{T}_h^4 (bottom left), \mathcal{T}_h^5 (bottom middle) and \mathcal{T}_h^6 (bottom right).

For the numerical schemes, we have used the lowest order of approximation $k = 0$. The order of convergence that we present in the forthcoming tables were obtained with a least-square fitting of the form

$$(5.1) \quad \omega_h \approx \omega_{\text{extr}} + Ch^\alpha,$$

where $\omega_h = \sqrt{\kappa_h}$ is the frequency computed with the method, $\omega_{\text{extr}} := \sqrt{\kappa_{\text{extr}}}$ is an extrapolated frequency given by the fitting, and α represents the order of convergence. The constant C is independent of the mesh-size.

On the tests, we aim, in one hand, compute the spectrum and convergence rates for the eigenvalues, and on the other, assess the the performance of the method with respect to the Poisson ratio ν . More precisely, recalling the definition of the Lamé constants

$$\lambda := \frac{E\nu}{(1+\nu)(1-2\nu)} \quad \text{and} \quad \mu := \frac{E}{2(1+\nu)},$$

where clearly, when $\nu \rightarrow 1/2$ the constant λ blows up. Hence, we aim to observe that the mixed scheme is locking free with respect to ν . In fact, when $\nu \rightarrow 1/2$, the bilinear form $a(\cdot, \cdot)$ must be modified in the sense that

$$(5.2) \quad a(\boldsymbol{\rho}, \boldsymbol{\tau}) := \frac{1}{\mu} \int_{\Omega} \boldsymbol{\rho}^{\text{d}} : \boldsymbol{\tau}^{\text{d}} \quad \forall \boldsymbol{\rho}, \boldsymbol{\tau} \in \mathbb{H}_0.$$

Hence, the computational code must be coherent with this modification.

Regarding the VEM scheme, as in [5], a choice for $S^E(\cdot, \cdot)$ is given by

$$S^E(\boldsymbol{\rho}_h, \boldsymbol{\tau}_h) := \gamma_E \sum_{k=1}^{N_E^k} m_{i,E}(\boldsymbol{\rho}_h) m_{i,E}(\boldsymbol{\tau}_h),$$

where the set $\{m_{i,E}(\boldsymbol{\rho}_h)\}_{i=1}^{N_E^k}$ corresponds to all the E -moments of $\boldsymbol{\rho}_h$ associated with degrees of freedom (3.1)–(3.3) and γ_E denotes the stability constant, which is assumed to be of order one.

The refinement parameter N used to label each mesh is the number of elements on each edge.

5.1. Test 1: The unit square. We begin by testing our method in the unit square $\Omega := (0, 1)^2$. The boundary condition for this test is $\mathbf{u} = 0$, that represents a clamped square. With this geometrical configuration, the eigenfunctions of the problems are sufficiently regular and hence, the order of convergence for the corresponding eigenvalues must be optimal.

We prove different meshes and different values of the Poisson ratio, particularly $\nu \in \{0.35, 0.49, 0.5\}$. Clearly $\nu = 0.5$ is the limit case where $\lambda = \infty$ implying that bilinear form (5.2) is the one that we consider for this case. In the following tables we report the obtained results. The parameter N is such that $N \sim h^{-1}$, α is the computed order obtained by (5.1) and the last column of each table presents the values obtained by the finite element method studied in [19].

TABLE 1
Test 1. Computed lowest eigenvalues ω_{hi} , $1 \leq i \leq 4$, on triangle meshes (\mathcal{T}_h^1).

$\nu = 0.35$						
ω_{hi}	$N = 16$	$N = 32$	$N = 64$	α	Extrap.	[19]
ω_{h1}	4.1220	4.1747	4.1884	1.93	4.1933	4.1931
ω_{h2}	4.1220	4.1747	4.1884	1.93	4.1933	4.1931
ω_{h3}	4.3086	4.3559	4.3681	1.96	4.3723	4.3722
ω_{h4}	5.7435	5.8829	5.9203	1.90	5.9340	5.9332
$\nu = 0.49$						
ω_{h1}	4.1248	4.1722	4.1845	1.95	4.1887	4.1886
ω_{h2}	5.3520	5.4748	5.5068	1.94	5.5180	5.5176
ω_{h3}	5.3520	5.4748	5.5068	1.94	5.5180	5.5176
ω_{h4}	6.3010	6.4797	6.5272	1.91	6.5445	6.5434
$\nu = 0.5$						
ω_{h1}	4.1132	4.1607	4.1730	1.95	4.1773	4.1771
ω_{h2}	5.3776	5.4991	5.5308	1.94	5.5419	5.5415
ω_{h3}	5.3776	5.4991	5.5308	1.94	5.5419	5.5415
ω_{h4}	6.2945	6.4735	6.5212	1.91	6.5384	6.5373

TABLE 2

Test 1. Computed lowest eigenvalues ω_{hi} , $1 \leq i \leq 4$, on hexagonal meshes. (\mathcal{T}_h^2).

$\nu = 0.35$						
ω_{hi}	$N = 16$	$N = 32$	$N = 64$	α	Extrap.	[19]
ω_{h1}	4.0653	4.1589	4.1843	1.88	4.1938	4.1931
ω_{h2}	4.0653	4.1589	4.1843	1.88	4.1938	4.1931
ω_{h3}	4.2719	4.3461	4.3656	1.93	4.3725	4.3722
ω_{h4}	5.6369	5.8512	5.9118	1.82	5.9358	5.9332
$\nu = 0.49$						
ω_{h1}	4.0880	4.1621	4.1819	1.91	4.1890	4.1886
ω_{h2}	5.2116	5.4357	5.4967	1.88	5.5194	5.5176
ω_{h3}	5.2116	5.4357	5.4967	1.88	5.5194	5.5176
ω_{h4}	6.1470	6.4366	6.5160	1.87	6.5458	6.5434
$\nu = 0.5$						
ω_{h1}	4.0763	4.1506	4.1704	1.91	4.1775	4.1771
ω_{h2}	5.2405	5.4609	5.5209	1.88	5.5432	5.5415
ω_{h3}	5.2405	5.4609	5.5209	1.88	5.5432	5.5415
ω_{h4}	6.1437	6.4311	6.5101	1.86	6.5403	6.5373

TABLE 3

Test 1. Computed lowest eigenvalues ω_{hi} , $1 \leq i \leq 4$, on distorted square meshes. (\mathcal{T}_h^3).

$\nu = 0.35$						
ω_{hi}	$N = 16$	$N = 32$	$N = 64$	α	Extrap.	[19]
ω_{h1}	4.0978	4.1678	4.1866	1.90	4.1934	4.1931
ω_{h2}	4.0991	4.1679	4.1866	1.87	4.1937	4.1931
ω_{h3}	4.3113	4.3560	4.3680	1.89	4.3725	4.3722
ω_{h4}	5.7201	5.8741	5.9178	1.82	5.9350	5.9332
$\nu = 0.49$						
ω_{h1}	4.1240	4.1711	4.1841	1.86	4.1890	4.1886
ω_{h2}	5.3046	5.4612	5.5031	1.90	5.5185	5.5176
ω_{h3}	5.3412	5.4716	5.5059	1.93	5.5180	5.5176
ω_{h4}	6.2785	6.4715	6.5247	1.86	6.5449	6.5434
$\nu = 0.5$						
ω_{h1}	4.1121	4.1594	4.1725	1.85	4.1776	4.1771
ω_{h2}	5.3352	5.4866	5.5274	1.89	5.5425	5.5415
ω_{h3}	5.3725	5.4972	5.5302	1.92	5.5420	5.5415
ω_{h4}	6.2742	6.4657	6.5187	1.85	6.5391	6.5373

TABLE 4

Test 1. Computed lowest eigenvalues ω_{hi} , $1 \leq i \leq 4$, on distorted square meshes. (\mathcal{T}_h^4).

$\nu = 0.35$						
ω_{hi}	$N = 9$	$N = 35$	$N = 61$	α	Extrap.	[19]
ω_{h1}	3.9389	4.1764	4.1876	2.00	4.1932	4.1931
ω_{h2}	3.9560	4.1766	4.1877	1.96	4.1932	4.1931
ω_{h3}	4.1836	4.3601	4.3682	2.02	4.3722	4.3722
ω_{h4}	5.3750	5.8926	5.9197	1.92	5.9339	5.9332
$\nu = 0.49$						
ω_{h1}	3.9941	4.1755	4.1843	1.98	4.1887	4.1886
ω_{h2}	5.0303	5.4859	5.5073	2.01	5.5177	5.5176
ω_{h3}	5.0720	5.4870	5.5075	1.97	5.5177	5.5176
ω_{h4}	5.8253	6.4912	6.5262	1.92	6.5443	6.5434
$\nu = 0.5$						
ω_{h1}	3.9818	4.1639	4.1728	1.98	4.1772	4.1771
ω_{h2}	5.0622	5.5104	5.5314	2.01	5.5417	5.5415
ω_{h3}	5.1134	5.5116	5.5316	1.95	5.5419	5.5415
ω_{h4}	5.8206	6.4850	6.5201	1.91	6.5387	6.5373

TABLE 5

Test 1. Computed lowest eigenvalues ω_{hi} , $1 \leq i \leq 4$, on hexagons (\mathcal{T}_h^5).

$\nu = 0.35$						
ω_{hi}	$N = 9$	$N = 35$	$N = 61$	α	Extrap.	[19]
ω_{h1}	3.9006	4.1724	4.1863	1.94	4.1934	4.1931
ω_{h2}	3.9257	4.1747	4.1871	1.97	4.1932	4.1931
ω_{h3}	4.1673	4.3583	4.3676	1.98	4.3722	4.3722
ω_{h4}	5.2953	5.8850	5.9172	1.88	5.9347	5.9332
$\nu = 0.49$						
ω_{h1}	3.9786	4.1736	4.1836	1.93	4.1888	4.1886
ω_{h2}	4.9504	5.4795	5.5051	1.98	5.5180.	5.5176
ω_{h3}	5.0553	5.4860	5.5071	1.97	5.5178.	5.5176
ω_{h4}	5.7675	6.4862	6.5244	1.90	6.5450.	6.5434
$\nu = 0.5$						
ω_{h1}	3.9664	4.1620	4.1721	1.93	4.1773	4.1771
ω_{h2}	4.9898	5.5043	5.5293	1.98	5.5418	5.5415
ω_{h3}	5.1024	5.5108	5.5313	1.95	5.5418	5.5415
ω_{h4}	5.7649	6.4800	6.5183	1.90	6.5387	6.5373

From Tables 1, 2, 3, 4, and 5 we observe that the double order of convergence predicted by Theorem 4.5 is attained in each case and is independent of the mesh under consideration, proving that the geometry does not affect the convergence rate. Additionally, the method is capable of capturing the spectrum of the problem for values of the Poisson ratio that includes the critical case $\nu = 0.5$, proving that the mixed VEM scheme is locking free. Finally, we observe that the extrapolated values that we obtain with our VEM method are close to those of [19]. In Figure 2 we display plots of some approximated eigenfunctions, obtained with different polygonal meshes.

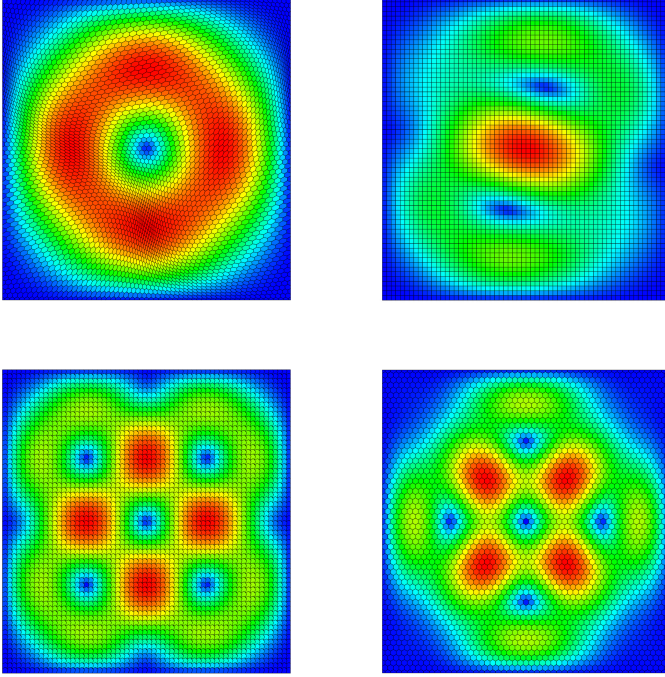


FIG. 2. *Test 1. Plots of the computed first eigenfunction for \mathcal{T}_h^4 (top left), second eigenfunction (top right) for \mathcal{T}_h^2 , fourth eigenfunction for \mathcal{T}_h^3 (bottom left) and fifth eigenfunction for \mathcal{T}_h^5 (bottom right).*

5.2. Test 2: L-shaped domain. In this test we consider a non-convex domain that we will call the L-shaped domain which is defined by $\Omega := (-1,1)^2 \setminus [-1,0]^2$. The importance of this geometry is that the geometrical singularity leads to non-sufficient smooth eigenfunctions for the elasticity eigenvalue problem. This is reflected on the numerical results when the order of convergence is computed. In the forthcoming tables we report the first five computed frequencies by our method for different meshes and different values of the Poisson ratio, the corresponding convergence rates, the extrapolated values, and the reference values that we use from reference [19].

TABLE 6

Test 2. Computed lowest eigenvalues ω_{hi} , $1 \leq i \leq 5$, on distorted square meshes. (\mathcal{T}_h^2).

$\nu = 0.35$							
ω_{hi}	$N = 8$	$N = 16$	$N = 32$	$N = 64$	α	Extrap.	[19]
ω_{h1}	2.2957	2.3530	2.3700	2.3756	1.72	2.3778	2.3783
ω_{h2}	2.6605	2.7587	2.7866	2.7946	1.81	2.7978	2.7976
ω_{h3}	3.0150	3.1920	3.2473	3.2680	1.62	3.2763	3.2777
ω_{h4}	3.3333	3.5383	3.5961	3.6147	1.79	3.6211	3.6215
ω_{h5}	3.4821	3.7011	3.7622	3.7803	1.83	3.7867	3.7866
$\nu = 0.49$							
ω_{h1}	2.9813	3.1669	3.2281	3.2530	1.53	3.2637	3.2661
ω_{h2}	3.1893	3.4154	3.4787	3.5005	1.78	3.5073	3.5085
ω_{h3}	3.4038	3.6302	3.6925	3.7108	1.84	3.7174	3.7172
ω_{h4}	3.6783	3.9394	4.0150	4.0356	1.80	4.0447	4.0427
ω_{h5}	3.7158	4.0670	4.1688	4.2007	1.77	4.2124	4.2125
$\nu = 0.5$							
ω_{h1}	2.9803	3.1682	3.2306	3.2563	1.52	3.2674	3.2699
ω_{h2}	3.1948	3.4200	3.4830	3.5047	1.78	3.5114	3.5126
ω_{h3}	3.4362	3.6541	3.7145	3.7324	1.83	3.7389	3.7388
ω_{h4}	3.6773	3.9374	4.0130	4.0336	1.80	4.0426	4.0408
ω_{h5}	3.8614	4.1650	4.2594	4.2863	1.71	4.2994	4.2968

TABLE 7

Test 2. Computed lowest eigenvalues ω_{hi} , $1 \leq i \leq 5$, on distorted square meshes. (\mathcal{T}_h^4).

$\nu = 0.35$							
ω_{hi}	$N = 9$	$N = 19$	$N = 35$	$N = 45$	α	Extrap.	[19]
ω_{h1}	2.3356	2.3668	2.3746	2.3759	1.74	2.3785	2.3783
ω_{h2}	2.7259	2.7798	2.7924	2.7944	1.83	2.7983	2.7976
ω_{h3}	3.1510	3.2407	3.2657	3.2698	1.60	3.2799	3.2777
ω_{h4}	3.4892	3.5882	3.6121	3.6156	1.80	3.6233	3.6215
ω_{h5}	3.6374	3.7510	3.7768	3.7805	1.88	3.7881	3.7866
$\nu = 0.49$							
ω_{h1}	3.1261	3.2217	3.2504	3.2555	1.48	3.2691	3.2661
ω_{h2}	3.3699	3.4718	3.4980	3.5017	1.72	3.5110	3.5085
ω_{h3}	3.5673	3.6814	3.7072	3.7110	1.88	3.7186	3.7172
ω_{h4}	3.8569	3.9984	4.0301	4.0350	1.89	4.0441	4.0427
ω_{h5}	3.9711	4.1497	4.1942	4.2010	1.75	4.2162.	4.2125
$\nu = 0.5$							
ω_{h1}	3.1264	3.2240	3.2535	3.2588	1.47	3.2729	3.2699
ω_{h2}	3.3752	3.4763	3.5022	3.5060	1.72	3.5152	3.5126
ω_{h3}	3.5981	3.7049	3.7293	3.7329	1.87	3.7401	3.7388
ω_{h4}	3.8551	3.9964	4.0281	4.0330	1.89	4.0421	4.0408.
ω_{h5}	4.0646	4.2380	4.2790	4.2857	1.81	4.2987	4.2968.

TABLE 8

Test 2. Computed lowest eigenvalues ω_{hi} , $1 \leq i \leq 5$, on distorted square meshes. (\mathcal{T}_h^5).

$\nu = 0.35$							
ω_{hi}	$N = 9$	$N = 19$	$N = 35$	$N = 45$	α	Extrap.	[19]
ω_{h1}	2.3341	2.3661	2.3743	2.3757	1.7000	2.3786	2.3783
ω_{h2}	2.7199	2.7777	2.7918	2.7940	1.7700	2.7987	2.7976
ω_{h3}	3.1351	3.2349	3.2638	3.2686	1.5400	3.2813	3.2777
ω_{h4}	3.4694	3.5817	3.6104	3.6144	1.7300	3.6245	3.6215
ω_{h5}	3.6209	3.7456	3.7753	3.7795	1.8200	3.7889	3.7866
$\nu = 0.49$							
ω_{h1}	3.1071	3.2145	3.2481	3.2539	1.4400	3.2705	3.2661
ω_{h2}	3.3423	3.4627	3.4954	3.5001	1.6500	3.5127	3.5085
ω_{h3}	3.5510	3.6756	3.7057	3.7100	1.8000	3.7197	3.7172
ω_{h4}	3.8433	3.9925	4.0282	4.0337	1.8000	4.0453	4.0427
ω_{h5}	3.9457	4.1421	4.1918	4.1994	1.7300	4.2168	4.2125
$\nu = 0.5$							
ω_{h1}	3.1062	3.2163	3.2510	3.2571	1.4200	3.2748	3.2699
ω_{h2}	3.3480	3.4673	3.4997	3.5043	1.6500	3.5168	3.5126
ω_{h3}	3.5807	3.6988	3.7277	3.7318	1.7800	3.7415	3.7388
ω_{h4}	3.8419	3.9905	4.0262	4.0318	1.8000	4.0432	4.0408
ω_{h5}	4.0510	4.2314	4.2766	4.2841	1.7300	4.2999	4.2968

We observe from Tables 6, 7, and 8 that our predictions are consistent with the theoretical results and the bibliography. On the one hand, the singularity precisely affects the regularity of some eigenfunctions, more precisely the first of them, since the convergence rate for the associated frequency is not optimal., whereas the rest of the frequencies are capable to be closed to the order $\mathcal{O}(h^2)$. Also, once again the results show that the method is locking free, since the limit case $\nu = 0.5$ behaves stable. Also, the choice of meshes does not affect the order of convergence for the frequencies, proving that the method is robust with respect to the geometry of the elements on the meshes. We end this test presenting some plots of the magnitude of the displacements for the first four eigenfunctions, computed with different polygonal meshes.

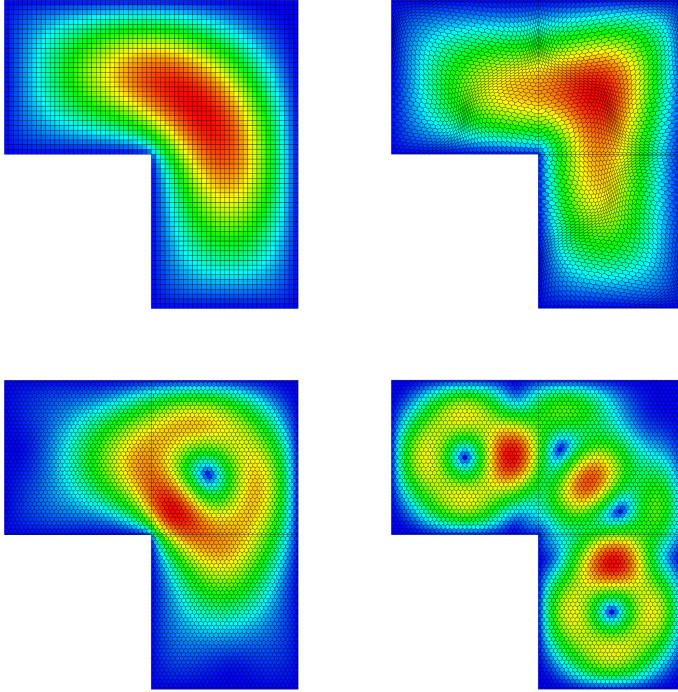


FIG. 3. *Test 2. Plots of the computed first eigenfunction for \mathcal{T}_h^2 (left), second eigenfunction (right) for \mathcal{T}_h^4 , third eigenfunction for \mathcal{T}_h^5 (bottom left) and fourth eigenfunction for \mathcal{T}_h^5 (bottom right). All these plots were obtained for $\nu = 0.49$.*

5.3. Test 3: Circular domain. The following test goes beyond the developed theory, since we assume a curved boundary. This clearly is not a suitable domain for our VEM, since we will approximate the boundary with polygons, leading to a variational crime. However, our intention is to show that the proposed method is capable to capture the spectrum of the elasticity eigenvalue problem despite this geometry. The computational domain consists in the unit circle defined by $\Omega =: \{(x, y) \in \mathbb{R}^2 : x^2 + y^2 < 1\}$. For this test we impose $\mathbf{u} = \mathbf{0}$ on $\partial\Omega$ as boundary condition. Since the domain is convex, we expect sufficiently smooth eigenfunctions for the problem and hence, quadratic order of convergence for the method.

TABLE 9

Test 3. Computed lowest eigenvalues ω_{hi} , $1 \leq i \leq 5$, on distorted square meshes. (\mathcal{T}_h^6).

$\nu = 0.35$							
ω_{hi}	$N = 115$	$N = 243$	$N = 357$	$N = 457$	α	Extrap.	[19]
ω_{h1}	2.3220	2.3301	2.3313	2.3316	2.1000	2.3322	2.33234
ω_{h2}	2.3222	2.3301	2.3313	2.3317	2.0200	2.3323	2.33190
ω_{h3}	2.3275	2.3309	2.3315	2.3317	1.8700	2.3320	2.33234
ω_{h4}	3.3033	3.3144	3.3162	3.3167	2.0000	3.3176	3.31761
ω_{h5}	3.3036	3.3145	3.3162	3.3167	1.9900	3.3176	3.31761
$\nu = 0.49$							
ω_{h1}	2.2154	2.2187	2.2192	2.2194	2.0100	2.2197	2.21964
ω_{h2}	2.9445	2.9550	2.9567	2.9572	1.9800	2.9581	2.95809
ω_{h3}	2.9447	2.9550	2.9567	2.9572	1.9600	2.9581	2.95809
ω_{h4}	3.6552	3.6767	3.6801	3.6812	2.0000	3.6829	3.68292
ω_{h5}	3.6563	3.6767	3.6801	3.6812	1.9300	3.6831	3.68292
$\nu = 0.5$							
ω_{h1}	2.2080	2.2113	2.2118	2.2120	2.0100	2.2122	2.21223
ω_{h2}	2.9519	2.9621	2.9637	2.9642	1.9800	2.9651	2.96505
ω_{h3}	2.9521	2.9621	2.9637	2.9642	1.9600	2.9651	2.96505
ω_{h4}	3.6563	3.6775	3.6808	3.6819	1.9900	3.6836	3.68358
ω_{h5}	3.6573	3.6775	3.6808	3.6819	1.9200	3.6838	3.68358

The results reported on Table 9 show that the VEM scheme is capable to capture the physical spectrum on a circular domain, for mesh \mathcal{T}_h^6 and for any value of the Poisson ratio. The results for other type of meshes are similar. It is clear that the orders of convergence convergence are the optimal for the selected values of ν , even for the limit case. We present in Figure 4 plots of the magnitude of the displacement of the first and fifth eigenfunctions.

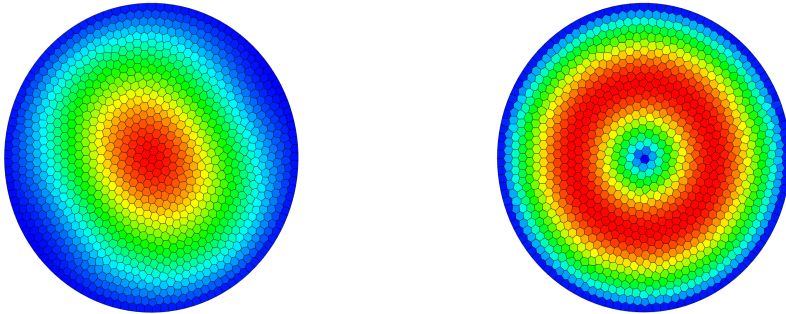


FIG. 4. Test 3. Plots of the computed first and the second eigenfunction for \mathcal{T}_h^6 and $\nu = 0.35$,

Remark 5.1. Since we are considering the lowest order approximation for the method ($k = 0$), it is not possible to observe the variational crime introduced by approximating curved boundaries with straight segments. If we implement a polynomial degree of approximation $k \geq 1$, this phenomenon would become evident as shown in [19] for the same domain.

5.4. Test 4: Effects of the stability constant γ_E . As a final test in this numerical section, we investigate the robustness of our method with respect to the stabilization parameter, in order to assess whether the quality of the computations and the accurate approximation of the operator spectrum may be affected by this constant. This type of behavior has already been observed in VEM solutions of different eigenvalue problems. In particular, it was shown in [33] that certain VEM discretizations of the Steklov eigenvalue problem introduce spurious eigenvalues, which can be suitably separated from the physical spectrum by an appropriate choice of the stability constant γ_E . Similar analyses, also carried out for instance in [3, 9, 23, 32] within the VEM framework, show analogous results. In the present case, no spurious eigenvalues were detected for any choice of this constant. This is due to the boundary condition $\mathbf{u} = \mathbf{0}$ imposed on the whole boundary $\partial\Omega$. However, for large values of γ_E , the eigenvalues computed on coarse meshes may exhibit very poor accuracy.

The scaled version of the stabilization term $S^E(\cdot, \cdot)$ is multiplied by a parameter γ_E , which is selected as follows: $\gamma_E = \{0, 2^{-6}, 2^{-3}, 1, 2^3, 2^6\}$. For this test, we have selected the mesh \mathcal{T}_h^2 , and the idea is to vary its refinement level in order to compute the eigenvalues using the fitting (5.1). For this purpose, the refinement is performed with $N = \{20, 60, 100, 140, 180\}$. Since $\Omega = (0, 1)^2$ and considering the physical parameters, we set $E = 1$ and the Poisson ratio $\nu = 0.49$. The results of this test are reported in Table 10.

TABLE 10

Test 4. Computed lowest eigenvalues ω_{hi} , $1 \leq i \leq 4$, on hexagonal meshes. (\mathcal{T}_h^2) for $\gamma_E = 0$ and $\gamma_E = 2^i$ with $i = \{-6, -3, 0, 3, 6\}$.

$\gamma_E = 0$							
ω_{hi}	$N = 20$	$N = 60$	$N = 100$	$N = 140$	$N = 180$	α	[19]
ω_{h1}	4.1227	4.1809	4.1858	4.1872	4.1877	2.0000	4.1886
ω_{h2}	5.3155	5.4938	5.5090	5.5132	5.5149	2.0018	5.5176
ω_{h3}	5.3155	5.4938	5.5090	5.5132	5.5149	2.0018	5.5176
ω_{h4}	6.2813	6.5123	6.5321	6.5376	6.5399	1.9983	6.5434
$\gamma_E = 2^{-6}$							
ω_{hi}	$N = 20$	$N = 60$	$N = 100$	$N = 140$	$N = 180$	α	[19]
ω_{h1}	4.1227	4.1809	4.1858	4.1872	4.1877	2.0000	4.1886
ω_{h2}	5.3155	5.4938	5.5090	5.5132	5.5149	2.0018	5.5176
ω_{h3}	5.3155	5.4938	5.5090	5.5132	5.5149	2.0018	5.5176
ω_{h4}	6.2813	6.5123	6.5321	6.5376	6.5399	1.9983	6.5434
$\gamma_E = 2^{-3}$							
ω_{hi}	$N = 20$	$N = 60$	$N = 100$	$N = 140$	$N = 180$	α	[19]
ω_{h1}	4.1227	4.1809	4.1858	4.1872	4.1877	2.0000	4.1886
ω_{h2}	5.3155	5.4938	5.5090	5.5132	5.5149	2.0018	5.5176
ω_{h3}	5.3155	5.4938	5.5090	5.5132	5.5149	2.0018	5.5176
ω_{h4}	6.2813	6.5123	6.5321	6.5376	6.5399	1.9983	6.5434
$\gamma_E = 2^0$							
ω_{hi}	$N = 20$	$N = 60$	$N = 100$	$N = 140$	$N = 180$	α	[19]
ω_{h1}	4.1227	4.1809	4.1858	4.1872	4.1877	2.0000	4.1886
ω_{h2}	5.3155	5.4938	5.5090	5.5132	5.5149	2.0018	5.5176
ω_{h3}	5.3155	5.4938	5.5090	5.5132	5.5149	2.0018	5.5176
ω_{h4}	6.2813	6.5123	6.5321	6.5376	6.5399	1.9983	6.5434
$\gamma_E = 2^3$							
ω_{hi}	$N = 20$	$N = 60$	$N = 100$	$N = 140$	$N = 180$	α	[19]
ω_{h1}	3.6366	4.1103	4.1596	4.1736	4.1795	2.0000	4.1886
ω_{h2}	4.1729	5.2869	5.4303	5.4724	5.4901	1.8951	5.5176
ω_{h3}	4.1729	5.2869	5.4303	5.4724	5.4901	1.8951	5.5176
ω_{h4}	4.7196	6.2472	6.4311	6.4852	6.5079	1.9189	6.5434
$\gamma_E = 2^6$							
ω_{hi}	$N = 20$	$N = 60$	$N = 100$	$N = 140$	$N = 180$	α	[19]
ω_{h1}	2.2721	3.6723	3.9722	4.0723	4.1165	2.0000	4.1886
ω_{h2}	2.3031	4.2499	4.9189	5.1816	5.3053	1.6583	5.5176
ω_{h3}	2.3031	4.2499	4.9189	5.1816	5.3053	1.6583	5.5176
ω_{h4}	2.3978	4.8192	5.7718	6.1121	6.2710	1.6711	6.5434

We observe from Table 10 that for small values of γ_E , the method is capable to attain optimal order of convergence as the theory predicts. Even if $\gamma_E = 1$ or $\gamma_E = 8$, the spectrum is correctly approximated. We have contrasted our results with the extrapolated values obtained in [19] for a FEM scheme. On the other hand, if the scaling parameter is larger, the order of convergence begins to deteriorate. Indeed, in the last row of Table 10, the first eigenvalue is approximated with optimal order, however the rest of the spectrum that we report, is not approximated with the expected order. Moreover, the eigenvalues computed with highly refined meshes are not similar to the reference values in [19]. These results are consistent with those

reported in [6, Table 4] where a similar phenomenon is observed.

REFERENCES

- [1] D. ADAK, G. MANZINI, AND S. NATARAJAN, *Nonconforming virtual element methods for velocity-pressure Stokes eigenvalue problem*, Appl. Numer. Math., 202 (2024), pp. 42–66, <https://doi.org/10.1016/j.apnum.2024.04.009>.
- [2] L. ALZABEN, D. BOFFI, A. DEDNER, AND L. GASTALDI, *On the stabilization of a virtual element method for an acoustic vibration problem*, Math. Models Methods Appl. Sci., 35 (2025), pp. 655–701, <https://doi.org/10.1142/S0218202525500071>.
- [3] D. AMIGO, F. LEPE, AND G. RIVERA, *A virtual element method for the elasticity spectral problem allowing for small edges*, J. Sci. Comput., 97 (2023), pp. Paper No. 54, 29, <https://doi.org/10.1007/s10915-023-02372-6>.
- [4] I. BABUŠKA AND J. OSBORN, *Handbook of numerical analysis. Vol. II*, (1991), pp. x+928. Finite element methods. Part 1.
- [5] L. BEIRÃO DA VEIGA, F. BREZZI, A. CANGIANI, G. MANZINI, L. D. MARINI, AND A. RUSSO, *Basic principles of virtual element methods*, Math. Models Methods Appl. Sci., 23 (2013), pp. 199–214, <https://doi.org/10.1142/S0218202512500492>.
- [6] L. C. BEIRÃO DA VEIGA, D. MORA, G. RIVERA, AND R. RODRÍGUEZ, *A virtual element method for the acoustic vibration problem*, Numer. Math., 136 (2017), pp. 725–763, <https://doi.org/10.1007/s00211-016-0855-5>.
- [7] D. BOFFI, *Finite element approximation of eigenvalue problems*, Acta Numer., 19 (2010), pp. 1–120, <https://doi.org/10.1017/S0962492910000012>.
- [8] D. BOFFI, F. BREZZI, AND M. FORTIN, *Mixed finite element methods and applications*, vol. 44 of Springer Series in Computational Mathematics, Springer, Heidelberg, 2013, <https://doi.org/10.1007/978-3-642-36519-5>.
- [9] D. BOFFI, F. GARDINI, AND L. GASTALDI, *Approximation of PDE eigenvalue problems involving parameter dependent matrices*, Calcolo, 57 (2020), pp. Paper No. 41, 21, <https://doi.org/10.1007/s10092-020-00390-6>.
- [10] D. BOFFI AND R. STENBERG, *A remark on finite element schemes for nearly incompressible elasticity*, Comput. Math. Appl., 74 (2017), pp. 2047–2055, <https://doi.org/10.1016/j.camwa.2017.06.006>.
- [11] E. CÁCERES AND G. N. GATICA, *A mixed virtual element method for the pseudostress-velocity formulation of the Stokes problem*, IMA J. Numer. Anal., 37 (2017), pp. 296–331, <https://doi.org/10.1093/imanum/drw002>.
- [12] E. CÁCERES, G. N. GATICA, AND F. A. SEQUEIRA, *A mixed virtual element method for the Brinkman problem*, Math. Models Methods Appl. Sci., 27 (2017), pp. 707–743, <https://doi.org/10.1142/S0218202517500142>.
- [13] E. CÁCERES, G. N. GATICA, AND F. A. SEQUEIRA, *A mixed virtual element method for a pseudostress-based formulation of linear elasticity*, Appl. Numer. Math., 135 (2019), pp. 423–442, <https://doi.org/10.1016/j.apnum.2018.09.003>.
- [14] C. CARSTENSEN, M. EIGEL, AND J. GEDICKE, *Computational competition of symmetric mixed FEM in linear elasticity*, Comput. Methods Appl. Mech. Engrg., 200 (2011), pp. 2903–2915, <https://doi.org/10.1016/j.cma.2011.05.013>.
- [15] G. N. GATICA, L. F. GATICA, AND F. A. SEQUEIRA, *A priori and a posteriori error analyses of a pseudostress-based mixed formulation for linear elasticity*, Comput. Math. Appl., 71 (2016), pp. 585–614, <https://doi.org/10.1016/j.camwa.2015.12.009>.
- [16] J. GOPALAKRISHNAN AND J. GUZMÁN, *Symmetric nonconforming mixed finite elements for linear elasticity*, SIAM J. Numer. Anal., 49 (2011), pp. 1504–1520, <https://doi.org/10.1137/10080018X>.
- [17] P. GRISVARD, *Problèmes aux limites dans les polygones. Mode d’emploi*, EDF Bull. Direction Études Rech. Sér. C Math. Inform., (1986), pp. 3, 21–59.
- [18] R. HIPTMAIR, *Finite elements in computational electromagnetism*, Acta Numer., 11 (2002), pp. 237–339, <https://doi.org/10.1017/S0962492902000041>.
- [19] D. INZUNZA, F. LEPE, AND G. RIVERA, *Displacement-pseudostress formulation for the linear elasticity spectral problem*, Numer. Methods Partial Differential Equations, 39 (2023), pp. 1996–2017, <https://doi.org/10.1002/num.22955>.
- [20] T. KATO, *Perturbation theory for linear operators*, Springer-Verlag, Berlin, 1995. Reprint of the 1980 edition.
- [21] F. LEPE, S. MEDDAHI, D. MORA, AND R. RODRÍGUEZ, *Mixed discontinuous Galerkin approximation of the elasticity eigenproblem*, Numer. Math., 142 (2019), pp. 749–786,

- <https://doi.org/10.1007/s00211-019-01035-9>.
- [22] F. LEPE AND G. RIVERA, *A priori error analysis for a mixed VEM discretization of the spectral problem for the Laplacian operator*, *Calcolo*, 58 (2021), pp. Paper No. 20, 30, <https://doi.org/10.1007/s10092-021-00412-x>.
- [23] F. LEPE AND G. RIVERA, *A virtual element approximation for the pseudostress formulation of the Stokes eigenvalue problem*, *Comput. Methods Appl. Mech. Engrg.*, 379 (2021), pp. Paper No. 113753, 21, <https://doi.org/10.1016/j.cma.2021.113753>.
- [24] S. MEDDAHI, *A DG method for a stress formulation of the elasticity eigenproblem with strongly imposed symmetry*, *Comput. Math. Appl.*, 135 (2023), pp. 19–30, <https://doi.org/10.1016/j.camwa.2023.01.022>, <https://doi-org.ezproxy.ubiobio.cl/10.1016/j.camwa.2023.01.022>.
- [25] S. MEDDAHI, D. MORA, AND R. RODRÍGUEZ, *Finite element spectral analysis for the mixed formulation of the elasticity equations*, *SIAM J. Numer. Anal.*, 51 (2013), pp. 1041–1063, <https://doi.org/10.1137/120863010>.
- [26] J. MENG AND L. MEI, *A mixed virtual element method for the vibration problem of clamped Kirchhoff plate*, *Adv. Comput. Math.*, 46 (2020), pp. Paper No. 68, 18, <https://doi.org/10.1007/s10444-020-09810-1>.
- [27] J. MENG AND L. MEI, *Virtual element method for the Helmholtz transmission eigenvalue problem of anisotropic media*, *Math. Models Methods Appl. Sci.*, 32 (2022), pp. 1493–1529, <https://doi.org/10.1142/S0218202522500348>.
- [28] J. MENG, L. MEI, AND M. FEI, \mathbf{H}^1 -conforming virtual element method for the Laplacian eigenvalue problem in mixed form, *J. Comput. Appl. Math.*, 436 (2024), pp. Paper No. 115395, 17, <https://doi.org/10.1016/j.cam.2023.115395>.
- [29] J. MENG, X. QIAN, F. SU, AND B.-B. XU, *Nitsche’s serendipity virtual element method for the eigenvalue problem*, *Comput. Methods Appl. Mech. Engrg.*, 446 (2025), pp. Paper No. 118336, 23, <https://doi.org/10.1016/j.cma.2025.118336>.
- [30] J. MENG, G. WANG, AND L. MEI, *Mixed virtual element method for the Helmholtz transmission eigenvalue problem on polytopal meshes*, *IMA J. Numer. Anal.*, 43 (2023), pp. 1685–1717, <https://doi.org/10.1093/imanum/drac019>.
- [31] J. MENG, Y. ZHANG, AND L. MEI, *A virtual element method for the Laplacian eigenvalue problem in mixed form*, *Appl. Numer. Math.*, 156 (2020), pp. 1–13, <https://doi.org/10.1016/j.apnum.2020.03.026>.
- [32] D. MORA AND G. RIVERA, *A priori and a posteriori error estimates for a virtual element spectral analysis for the elasticity equations*, *IMA J. Numer. Anal.*, 40 (2020), pp. 322–357, <https://doi.org/10.1093/imanum/dry063>.
- [33] D. MORA, G. RIVERA, AND R. RODRÍGUEZ, *A virtual element method for the Steklov eigenvalue problem*, *Math. Models Methods Appl. Sci.*, 25 (2015), pp. 1421–1445, <https://doi.org/10.1142/S0218202515500372>, hdl.handle.net/10533/148013.
- [34] G. WANG, J. MENG, Y. WANG, AND L. MEI, *A priori and a posteriori error estimates for a virtual element method for the non-self-adjoint Steklov eigenvalue problem*, *IMA J. Numer. Anal.*, 42 (2022), pp. 3675–3710, <https://doi.org/10.1093/imanum/drab079>.
- [35] X. ZHONG AND W. QIU, *Spectral analysis of a mixed method for linear elasticity*, *SIAM J. Numer. Anal.*, 61 (2023), pp. 1885–1917, <https://doi.org/10.1137/22M148611X>.